

**DEVELOPMENT AND EVALUATION OF A SOLAR
PHOTO VOLTAIC ASSISTED SPRAYER MOUNTED ON A
SELF PROPELLED CARRIER**

Thesis

**Submitted to the Punjab Agricultural University
in partial fulfillment of the requirements
for the degree of**

**MASTER OF TECHNOLOGY
in
FARM MACHINERY AND POWER ENGINEERING
(Minor Subject: Energy Science and Technology)**

By

**Tushar Dhar
(L-2018-AE-185-M)**

**Department of Farm Machinery and Power Engineering
College of Agricultural Engineering and Technology
©PUNJAB AGRICULTURAL UNIVERSITY
LUDHIANA-141 004
2021**

CERTIFICATE - I

This is to certify that the thesis entitled, “**Development and evaluation of a solar photo voltaic assisted sprayer mounted on a self propelled carrier**” submitted for the degree of **Master of Technology**, in the subject of **Farm Machinery and Power Engineering** (Minor subject: **Energy Science and Technology**) of the Punjab Agricultural University, Ludhiana, is a bonafide research work carried out by **Tushar Dhar (L-2018-AE-185-M)** under my supervision and that no part of this thesis has been submitted for any other degree.

The assistance and help received during the course of investigation have been fully acknowledged.

(Er. Rajesh Soni)
Major Advisor
Associate Professor
Deptt. of Farm Machinery and Power
Engineering
Punjab Agricultural University
Ludhiana-141004

CERTIFICATE -II

This is to certify that the thesis entitled, “**Development and evaluation of a solar photo voltaic assisted sprayer mounted on a self propelled carrier**” submitted by **Tushar Dhar (L-2018-AE-185-M)** to the Punjab Agricultural University, Ludhiana in partial fulfilment of the requirements for the degree of **Master of Technology**, in the subject of **Farm Machinery and Power Engineering** (Minor subject: **Energy Science and Technology**) has been approved by the Student’s Advisory Committee along with Head of the Department after an oral examination on the same.

(Er. Rajesh Soni)
Major Advisor

(Dr Adarsh Kumar)
External Examiner
Principal Scientist
Division of Agricultural Engineering,
IARI, Pusa, New Delhi -110012

(Dr. Mahesh Kumar Narang)
Head of Department

(Dr. Jaskarn Singh Mahal)
Dean, Post Graduate Studies

ACKNOWLEDGEMENTS

I have been able to bring this study in the present shape only because of heartily cooperation of number of heads and hands. There are some who have blessed, some who assisted and some who have supplemented. I owe my gratitude to Punjab Agricultural University for providing me an opportunity to undergo this M.Tech. programme.

*I feel great pleasure to place on record my deep sense of appreciation and heartfelt thanks to my major advisor **Er. Rajesh Soni**, Associate Professor, Department of Farm Machinery and Power Engineering. My advisor's profound experience, positive approach, efficacious advice, constructive criticism, critical suggestions, constant encouragement, immense help and sympathetic attitude have stood me in good stead throughout my research work. I express my trust and soul felt gratitude to him for shaping and completing this task.*

*I am very grateful to **Dr. Manjeet Singh**, Principal Scientist, Department of Farm Machinery and Power Engineering for providing necessary facilities for successful completion of this work. His positive attitude and regular enquiry throughout the period is notable.*

*It is my profound privilege to express ineffable and deep sense of gratitude to members of my advisory committee **Dr. S.K. Singh**, Principal Scientist, Department of Renewable Energy Engineering, **Dr. Rohinish Khurana** (Dean PGS Nominee) Professor, Department of Farm Machinery and Power Engineering, **Dr. Derminder Singh**, Professor, Department of Electrical Engineering and Information Technology and **Dr. Sukhmeet Singh**, Head, Department of Mechanical Engineering for their excellent help and valuable guidance throughout the course of my study.*

*I would also like to express my gratitude to **Dr. Anoop Kumar Dixit**, Principal Scientist, Department of Farm Machinery and Power Engineering for providing the necessary man power and components during fabrication of the machine.*

*I express heartiest thanks to my seniors **Er. Susanta, Er. Avesh, Mr. Atin and Er. Raghuvir Parmar**. I am extremely thankful to my batchmates **Tapas, Amritpal, Ashley, Ramrang, Biswa, Ashish** and my juniors **Aashvi, Dipika, Neetika and Vishal**.*

*Above all, I would like to thank my parents **Mr. Parimal Kumar Dhar and Mrs. Bina Dhar** and my brother **Tanmay** for supporting me throughout my years of education, both morally and financially and for their love and inspiration in my life.*

Everybody may not have been mentioned, but none is forgotten. To all of them, I express my heartfelt and sincere thanks.

(Tushar Dhar)

Title of the Thesis	: Development and evaluation of a solar photo voltaic assisted sprayer mounted on a self propelled carrier
Name of the Student and Admission No.	: Tushar Dhar L-2018-AE-185-M
Major Subject	: Farm Machinery and Power Engineering
Minor Subject	: Energy Science and Technology
Name and Designation of Major Advisor	: Er. Rajesh Soni Associate Professor
Degree to be awarded	: M.Tech.
Year of award of Degree	: 2021
Total Pages in thesis	: 64 + Appendices (i-ix) + VITA
Name of the University	: Punjab Agricultural University, Ludhiana-141 004, Punjab, India

ABSTRACT

India is gifted with a vast potential in solar energy. Punjab has an average annual solar radiation is about 5.32 kWh/m²/day. This can be utilized to produce electricity using solar photo voltaic (SPV) system for running various farm devices/operations. A SPV assisted sprayer mounted on a self propelled carrier was developed which uses solar energy to charge the battery which simultaneously operates the spray pump while the carrier was engine operated. Selection of solar panels was based on the solar radiation availability during the winter season in Ludhiana, Punjab. Hollow cone nozzles were selected for the sprayer. This was tested at pressures (2, 3 and 4 kg/cm²) and heights (45, 50 and 55 cm) in a patternator for selection of best operational parameters for evaluation of field and spray parameters. The sprayer was operated at two forward speeds (0.6 and 0.7 m/s) in wheat. The application rate of the sprayer was 156.23 l/ha at forward speed of 0.6 m/s which was within the recommended application rate for aphids in wheat. The actual field capacity was 0.49 ha/h and 0.59 ha/h at forward speeds of 0.6 m/s and 0.7 m/s respectively. The field efficiency of the developed sprayer was about 75-80%. Spray parameters were determined at two different locations of the canopy (top and middle). Smaller droplets were observed at higher pressure. Uniformity coefficient varied from 1.59-2.32. Pressure and forward speed had a significant effect on the droplet density. The droplet density and spray coverage area was lesser at the under side of the leaves compared to the upper side of leaves. Ground losses decreased with the increase in nozzle pressure.

Keywords: Solar photo voltaic, SPV assisted sprayer, Self propelled carrier, Droplet density, Spray coverage area

Signature of Major Advisor

Signature of the Student

ਥੀਸਿਜ਼ ਦਾ ਸਿਰਲੇਖ	: ਸਵੈ ਚਲਿਤ ਕੈਰੀਅਰ ਤੇ ਲਗਾਏ ਗਏ ਸੋਲਰ ਫੋਟੋ ਵੋਲਟਿਕ ਸਹਾਇਤਾ ਨਾਲ ਚੱਲਣ ਵਾਲੇ ਸਪਰੇਅਰ ਦਾ ਵਿਕਾਸ ਅਤੇ ਮੁਲਾਂਕਣ
ਵਿਦਿਆਰਥੀ ਦਾ ਨਾਮ ਅਤੇ ਦਾਖਲਾ ਨੰਬਰ	: ਤੁਸ਼ਾਰ ਧਰ ਐਲ-2018-ਏ.ਈ.-185-ਐਮ
ਮੁੱਖ ਵਿਸ਼ਾ	: ਫਾਰਮ ਮਸ਼ੀਨਰੀ ਅਤੇ ਪਾਵਰ ਇੰਜੀਨੀਅਰਿੰਗ
ਸਹਿਯੋਗੀ ਵਿਸ਼ਾ	: ਐਨਰਜੀ ਸਾਇੰਸ ਅਤੇ ਤਕਨਾਲੋਜੀ
ਮੁੱਖ ਸਲਾਹਕਾਰ ਦਾ ਨਾਮ ਅਤੇ ਅਹੁੱਦਾ	: ਇੰਜ. ਰਾਜੇਸ਼ ਸੋਨੀ ਸਹਿਯੋਗੀ ਪ੍ਰੋਫੈਸਰ
ਡਿਗਰੀ ਦਾ ਨਾਮ	: ਐਮ. ਟੈਕ.
ਡਿਗਰੀ ਨਾਲ ਸਨਮਾਨਿਤ ਕਰਨ ਦਾ ਸਾਲ	: 2021
ਖੋਜ ਪੱਤਰ ਦੇ ਕੁੱਲ ਪੰਨੇ	: 64 + ਅੰਤਿਕਾ (i-ix) + ਵੀਟਾ
ਯੂਨੀਵਰਸਿਟੀ ਦਾ ਨਾਮ	: ਪੰਜਾਬ ਖੇਤੀਬਾੜੀ ਯੂਨੀਵਰਸਿਟੀ, ਲੁਧਿਆਣਾ 141004, ਪੰਜਾਬ, ਭਾਰਤ

ਸਾਰ

ਕੁਦਰਤੀ ਤੌਰ ਤੇ ਭਾਰਤ ਵਿੱਚ ਭਰਪੂਰ ਮਾਤਰਾ ਵਿੱਚ ਸੂਰਜੀ ਊਰਜਾ ਮਿਲਦੀ ਹੈ। ਪੰਜਾਬ ਵਿੱਚ ਔਸਤਨ ਸਲਾਨਾ ਸੌਰ ਊਰਜਾ ਤਕਰੀਬਨ $5.32 \text{ kWh/m}^2/\text{day}$ ਹੈ। ਇਹ ਸੋਲਰ ਵੋਲਟਿਕ ਸਿਸਟਮ ਰਾਹੀਂ ਬਿਜਲੀ ਪੈਦਾ ਕਰਕੇ ਖੇਤੀਬਾੜੀ ਸੰਦਾਂ ਨੂੰ ਚਲਾਉਣ ਦੇ ਕੰਮ ਲਿਆਂਦੀ ਜਾ ਸਕਦੀ ਹੈ। ਸਵੈ ਚਲਿਤ ਕੈਰੀਅਰ ਤੇ ਲਗਾਏ ਗਏ ਸੋਲਰ ਫੋਟੋ ਵੋਲਟਿਕ ਸਹਾਇਤਾ ਨਾਲ ਚੱਲਣ ਵਾਲੇ ਸਪਰੇਅਰ ਦਾ ਵਿਕਾਸ ਕੀਤਾ ਗਿਆ। ਇਸ ਵਿੱਚ ਸੌਰ ਊਰਜਾ ਦੁਆਰਾ ਬੈਟਰੀ ਨੂੰ ਚਾਰਜ ਕੀਤਾ ਜਾਂਦਾ ਹੈ ਅਤੇ ਸਪਰੇਅਰ (ਸੰਦ) ਨੂੰ ਖੇਤ ਵਿੱਚ ਇੰਜਨ ਦੀ ਸਹਾਇਤਾ ਨਾਲ ਚਲਾਇਆ ਜਾਂਦਾ ਹੈ। ਸੌਰ ਪੈਨਲ ਦਾ ਚੁਣਾਵ ਲੁਧਿਆਣਾ ਵਿਖੇ ਸਰਦੀਆਂ ਦੇ ਮੌਸਮ ਦੀ ਸੌਰ ਊਰਜਾ ਦੀ ਉਪਲਬਧਤਾ ਦੇ ਅਧਾਰ ਤੇ ਕੀਤਾ ਗਿਆ। ਸਪਰੇਅਰ ਵਾਸਤੇ ਖੋਖਲੇ ਕੋਨ ਦੀ ਨੋਜ਼ਲ ਦਾ ਚੁਣਾਵ ਕੀਤਾ ਗਿਆ। ਉਸ ਦਾ ਪ੍ਰੀਖਣ ਦਬਾਅ (2, 3 ਅਤੇ 4 kg/cm^2) ਅਤੇ ਉਚਾਈ (45, 50 and 55 cm) ਪੈਟਰਨੇਟਰ ਵਿੱਚ ਖੇਤ ਵਿੱਚ ਸਪਰੇ ਮਾਪਦੰਡ ਨਿਰਧਾਰਤ ਕਰਨ ਹਿਤ ਕੀਤਾ ਗਿਆ। ਕਣਕ ਦੀ ਫਸਲ ਵਿੱਚ ਸਪਰੇਅਰ ਨੂੰ ਦੋ ਗਤੀਆਂ (0.6 and 0.7 m/s) ਤੇ ਚਲਾਇਆ ਗਿਆ। ਸਪਰੇਅਰ ਦੀ ਸਪਰੇ ਕਰਨ ਦੀ ਸਮਰੱਥਾ 156.23 l/ha ਅਤੇ 0.6 m/s ਦੀ ਗਤੀ, ਜਿਹੜੀ ਕਿ ਕਣਕ ਦੀ ਫਸਲ ਵਿੱਚ ਏਫਿਡ ਤੇ ਸਪਰੇ ਦੀ ਮਾਤਰਾ ਦੀ ਸਿਫਾਰਸ਼ ਮਾਤਰਾ ਦੇ ਅੰਤਰਗਤ ਹੀ ਸੀ। ਅਸਲ ਵਿੱਚ ਖੇਤ ਵਿੱਚ ਸਪਰੇਅਰ ਦੀ ਸਮਰੱਥਾ ਕਰਮਵਾਰ 0.49 ha/h ਅਤੇ 0.59 ha/h ਜਿਹੜੀ ਕਿ 0.6 m/s and 0.7 m/s ਤੇ ਨਾਪੀ ਗਈ। ਖੇਤ ਵਿੱਚ ਇਸ ਸਪਰੇਅਰ ਦੀ ਕਾਰਜਕੁਸ਼ਲਤਾ 75– 80% ਦੇ ਲੱਗਭੱਗ ਸੀ। ਸਪਰੇ ਮਾਪਦੰਡ ਦੇ ਵੱਖ ਵੱਖ ਜਗ੍ਹਾ ਤੇ ਕਣਕ ਦੇ ਬੂਟਿਆਂ ਦੇ ਉਪਰਲੇ ਹਿੱਸੇ ਅਤੇ ਮਧਲੇ ਹਿੱਸੇ ਤੇ ਸਪਰੇ ਕਰਕੇ ਨਿਰਧਾਰਤ ਕੀਤੇ ਗਏ। ਵੱਧ ਦਬਾਅ ਤੇ ਜਿਆਦਾ ਛੋਟੀਆਂ ਛੋਟੀਆਂ ਸਪਰੇ ਦੀ ਬੂੰਦਾਂ ਨਜ਼ਰ ਆਈਆਂ। ਇਕਸਾਰਤਾ ਗੁਣਾਂਕ 1.59 ਤੋਂ 2.32 ਰਿਹਾ। ਦਬਾਅ ਅਤੇ ਸਪਰੇਅਰ ਦੀ ਗਤੀ ਦਾ ਬੂੰਦਾਂ ਦੀ ਗਣਤਾ ਤੇ ਮਹੱਤਵਪੂਰਨ ਪ੍ਰਭਾਵ ਪਿਆ। ਸਪਰੇਅਰ ਦੀ ਵਿਆਪਤੀ ਸਮਰੱਥਾ ਕਣਕ ਦੇ ਬੂਟਿਆਂ ਦੇ ਉਪਰਲੇ ਹਿੱਸੇ ਦੇ ਮੁਕਾਬਲੇ ਨਿਚਲੇ ਹਿੱਸੇ ਵਿੱਚ ਸਪਰੇ ਬੂੰਦਾਂ ਦੀ ਘਣਤਾ ਘੱਟ ਨਜ਼ਰ ਆਈ। ਨੋਜ਼ਲ ਦਾ ਦਬਾਅ ਵਧਣ ਨਾਲ ਸਪਰੇ ਦਾ ਜ਼ਮੀਨੀ ਨੁਕਸਾਨ ਘੱਟ ਪਾਇਆ ਗਿਆ।

ਮੁੱਖ ਸ਼ਬਦ: ਸੌਰ ਫੋਟੋ ਵੋਲਟੇਕ, ਸੌਰ ਫੋਟੋ ਵੋਲਟੇਕ ਦੀ ਸਹਾਇਤਾ ਨਾਲ ਚੱਲਣ ਵਾਲਾ ਸਪਰੇਅਰ, ਸਵੈਚਲਿਤ ਕੈਰੀਅਰ, ਬੂੰਦਾਂ ਦੀ ਘਣਤਾ, ਸਪਰੇ ਵਿਆਪਤੀ ਖੇਤਰ।

CONTENTS

Chapter	Topic	Page
	LIST OF TABLES	
	LIST OF FIGURES	
	LIST OF ABBREVIATIONS	
I	INTRODUCTION	1-2
II	REVIEW OF LITERATURE	3-10
	2.1 Solar energy and its applications in sprayers	3
	2.2 Laboratory and field evaluation of sprayers	6
III	MATERIAL AND METHODS	11-34
	3.1 Development of the solar photovoltaic assisted sprayer	11
	3.1.1 Solar power potential	11
	3.1.2 Selection of motor	12
	3.1.3 Selection of battery	12
	3.1.4 Selection of the solar PV panels	13
	3.1.5 Selection of solar charge controller	14
	3.1.6 Selection of the nozzles	15
	3.1.6.1 Study of the nozzle characteristics	15
	3.1.6.1.1 Patternator	16
	3.1.6.1.2 Discharge rate	16
	3.1.6.1.3 Spray angle	17
	3.1.6.1.4 Swath width	17
	3.1.6.1.5 Spray distribution pattern	17
	3.1.6.2 Nozzle spacing	17
	3.1.7 Initial testing of the solar PV assisted sprayer	17
	3.1.8 Assembly of parts for solar PV assisted sprayer	19
	3.2 Development of the self propelled carrier for mounting the spraying assembly	20
	3.3 Performance evaluation of the solar photovoltaic assisted sprayer mounted on a self	24

	propelled carrier	
3.3.1	Performance evaluation of the solar PV setup	24
3.3.1.1	Array output	26
3.3.1.2	Efficiency of PV panel or conversion efficiency	26
3.3.2	Field evaluation of the SPV assisted sprayer mounted on a self propelled carrier	26
3.3.2.1	Field parameters	28
3.3.2.1.1	Swath width	28
3.3.2.1.2	Application rate	28
3.3.2.1.3	Field capacity	28
3.3.2.1.4	Field efficiency	29
3.3.2.2	Spray parameters	29
3.3.2.2.1	Droplet size	33
3.3.2.2.2	Droplet deposition	34
3.4	Statistical analysis	34
IV	RESULTS AND DISCUSSION	35-55
4.1	Laboratory evaluation of the hollow cone nozzle	35
4.1.1	Nozzle characteristics	35
4.1.1.1	Rate of discharge	35
4.1.1.2	Spray angle	35
4.1.1.3	Swath width	36
4.1.1.4	Spray distribution pattern	37
4.1.2	Nozzle spacing	38
4.2	Performance evaluation of the solar PV setup	39
4.2.1	Variation of array output with solar irradiance	40
4.2.2	Variation of ambient temperature and panel temperature with time	40
4.2.3	Variation of conversion efficiency with panel temperature	40
4.3	Field evaluation of the SPV assisted sprayer	42

	mounted on a self propelled carrier	
4.3.1	Field parameters	42
4.3.1.1	Swath width	42
4.3.1.2	Application rate	42
4.3.1.3	Field capacity	43
4.3.1.4	Field efficiency	43
4.3.2	Spray parameters	44
4.3.2.1	Droplet size and uniformity coefficient	44
4.3.2.1.1	Number median diameter (NMD)	44
4.3.2.1.1.1	NMD at top canopy of wheat	44
4.3.2.1.1.2	NMD at middle canopy of wheat	45
4.3.2.1.2	Volume median diameter (VMD)	46
4.3.2.1.2.1	VMD at top canopy of wheat	46
4.3.2.1.2.2	VMD at middle canopy of wheat	47
4.3.2.1.3	Uniformity coefficient (UC)	48
4.3.2.1.3.1	UC at top canopy of wheat	48
4.3.2.1.3.2	UC at middle canopy of wheat	49
4.3.2.2	Spray deposition	50
4.3.2.2.1	Droplet density	50
4.3.2.2.1.1	Droplet density at top canopy of wheat	50
4.3.2.2.1.2	Droplet density at middle canopy of wheat	51
4.3.2.2.2	Spray coverage area (%)	52
4.3.2.2.2.1	Spray coverage area (%) at top canopy of wheat	52
4.3.2.2.2.1	Spray coverage area(%) at middle canopy of wheat	53
4.3.2.2.3	Ground losses	54
V	SUMMARY	56-59
	SUGGESTIONS FOR FUTURE WORK	60
	REFERENCES	61-64
	APPENDICES	i-ix
	VITA	

LIST OF TABLES

Table No.	Title	Page No.
3.1	Specifications of each diaphragm pump motor	12
3.2	Levels of independent and dependent parameters used for laboratory study	16
3.3	Specifications of each solar panel	19
3.4	Specifications of the diesel engine	21
3.5	Levels of independent and dependent parameters used for field evaluation	27
4.1	Effect of different pressures and nozzle heights on swath width	36
4.2	Minimum CV at different pressures and nozzle heights	38
4.3	Recorded observations on 30 January 2021	39
4.4	Total and average discharge from the nozzles of boom	42
4.5	Field capacities at different forward speeds and number of nozzles	43
4.6	NMD (μm) at top canopy of wheat	44
4.7	Significance of pressure and forward speed on NMD at top canopy	45
4.8	NMD (μm) at middle canopy of wheat	45
4.9	Significance of pressure and forward speed on NMD at middle canopy	46
4.10	VMD (μm) at top canopy of wheat	46
4.11	Significance of pressure and forward speed on VMD at top canopy	47
4.12	VMD (μm) at middle canopy of wheat	47
4.13	Significance of pressure and forward speed on VMD at middle canopy	48
4.14	UC at top canopy of wheat	48

4.15	Significance of pressure and forward speed on UC at top canopy	49
4.16	UC at middle canopy of wheat	49
4.17	Significance of pressure and forward speed on UC at middle canopy	49
4.18	Droplet density at top canopy of wheat	50
4.19	Significance of pressure and forward speed on droplet density at top canopy	51
4.20	Droplet density at middle canopy of wheat	51
4.21	Significance of pressure and forward speed on droplet density at middle canopy	52
4.22	Coverage area (%) at top canopy of wheat	53
4.23	Significance of pressure and forward speed on coverage area at top canopy	53
4.24	Coverage area (%) at middle canopy of wheat	54
4.25	Significance of pressure and forward speed on coverage area at middle canopy	54
4.26	Ground losses	55
4.27	Significance of pressure and forward speed on ground losses	55

LIST OF FIGURES

Figure No.	Title	Page No.
3.1	Map showing global horizontal irradiation in India	11
3.2	Diaphragm pump motor	12
3.3	Solar charge controller	15
3.4	Hollow cone nozzle	15
3.5	Spray patternator	16
3.6	Initial testing of the spray boom using battery	17
3.7	Lead acid battery	18
3.8	Solar panel	18
3.9	Circuit diagram of the SPV assisted spraying system	19
3.10	Initial view of the available frame	20
3.11	3D view of the machine	22
3.12	2D conceptual views of the machine	23
3.13	Actual view of the developed machine	24
3.14	Recording of panel temperature and solar radiation	25
3.15	Solar power meter	25
3.16	Infrared thermometer	25
3.17	Field operation of the solar photovoltaic assisted sprayer mounted on a self propelled carrier	27
3.18	Stands holding water sensitive papers in wheat crop	29
3.19	Interface of DepositScan software	31
3.20	Scanning of water sensitive papers using scanner	32
3.21	Image processing in DepositScan software	32
4.1	Effect of different pressures on discharge	35
4.2	Effect of different pressures on angle of spray	36

4.3	Spray distribution at 45 cm nozzle height	37
4.4	Spray distribution at 50 cm nozzle height	37
4.5	Spray distribution at 55 cm nozzle height	38
4.6	Variation of solar irradiance and array output with time	41
4.7	Variation of array output, panel temperature and conversion efficiency with time	41
4.8	Discharge variation from every nozzles of boom	43

LIST OF ABBREVIATIONS

%	:	percentage
µl	:	microlitre
°	:	degrees
C	:	Celsius
A	:	ampere
Ah	:	ampere hour
ANOVA	:	Analysis of Variance
cm	:	centimeter
cm ²	:	square centimeter
COAE&T	:	College of Agricultural Engineering & Technology
CV	:	Coefficient of variation
DC	:	Direct current
et al	:	Et alibi
etc	:	Et-cetera
Fig	:	Figure
FM&PE	:	Farm Machinery & Power Engineering
h	:	hour
ha	:	hectare
i.e.	:	that is
kg	:	kilogram
km/h	:	kilometre per hour
kPa	:	kilopascal
kW	:	kilo watt
l	:	litre
m	:	metre
mm	:	millimetre
ml	:	millilitre
m/s	:	metre per second
PAU	:	Punjab Agricultural University
s	:	second
sq	:	square
V	:	voltage
W	:	watt
Wp	:	watt peak

CHAPTER I

INTRODUCTION

Energy is a vital input for the growth of economy and development of any country (Aju *et al* 2016). Large quantities of fossil fuels have been expended, and harmful emissions are being released into the environment by automobiles, especially in recent decades (Lu *et al* 2011). In India, fossil fuel demand is very high, which leads to large amount of imports nearly 84% of fuel requirement (Anonymous 2019a). This very high amount of import of fossil fuels affects the foreign exchange and results in increment of prices of the fossil fuels (Swaminathan *et al* 2010). Also, global climate change is one of the significant environmental concerns in the current scenario. The only way to overcome or to lessen this disaster is to mitigate the level of greenhouse gases (Dawn *et al* 2016). Hence, the public interest is increasing in alternative energy resources (solar, wind, biomass etc.) to fulfil the energy demand as well as to reduce the emissions of greenhouse gases.

Solar energy has been widely tipped to be the next major sustainable energy resource. It is a clean, renewable, everlasting energy source having no potential damage on the environment. The amount of solar radiation reaching the earth's surface is roughly equal to 1000 W/m^2

India is gifted with a vast potential in solar energy. Solar energy of around 4 to 7 kWh/m² per day is available on India's soil with a range of global radiation around 1700 to 2300 kWh/m² annually (Chandra *et al* 2019). In Punjab region, the average annual solar radiation is about 5.32 kWh/m²/day (Singh *et al* 2013). Thus a huge amount of solar energy is available in India which can be utilized to generate heat or electricity through suitable methods.

Sun's energy can be used for generating electricity using solar photovoltaics (SPV). Demand of electricity in India is increasing at a very fast rate due to economic development and population growth. It was observed that, according to census of India, in 2011, only 55.5% of rural households had access to electricity (Chandra *et al* 2019). Hence, SPV is an important asset in today's world, which is being widely used for generation of electricity. Apart from electrification, vehicular operations are now slowly moving towards solar energy.

Farm machinery plays an important role in agricultural operations. Presently, the major source of energy input/supply to the power source of these tools/implements/machines is diesel or petrol. The total diesel consumption in completing all the tillage, planting/transplanting, spraying and combine harvesting operations in wheat-paddy cycle is approximately 181.6 l/ha. In order to reduce dependency on fossil fuels and cost of various farm operations, one alternative is the use of solar energy to replace the use of fossil fuel. The solar radiation is abundantly available and the electricity produced from solar photovoltaic (SPV) system can be used to power various farm devices/operations.

One of the important operation in agricultural field is plant protection using sprayers or dusters. Indian farms generally use two types of spraying pumps, which are fuel operated and hand operated type, among which hand operated spraying pumps are most prevalent (Mishra *et al* 2019). But hand operated sprayer leads to higher human efforts during the operation, as a result it leads to discomfort and the operator cannot continue for a longer time. Diesel or petrol operated sprayers minimize the human drudgery but the limitation is its higher cost of operation due to the fuel used and also emission of various pollutant gases which leads to environmental issues. Electrical sprayers are operated on electricity for charging the battery which drives the pump (Chandrashekar *et al* 2018). Hence, the technology of solar energy can be extended for spraying pesticides, fungicides, fertilizers, nutrients and weedicides using solar sprayers (Joshua *et al* 2010).

As of now the solar operated sprayers which have been developed has basically been backpack type or manual push type. However, these types of sprayers increases the drudgery on the operator when it is to be operated for a longer period of time or for a whole day of operation. Also, the capacity of the backpack and manual push types is very low. Self propelled boom type sprayers which have been developed in the past were basically operated using diesel engines.

Hence, to overcome these drawbacks, a SPV assisted sprayer mounted on a self propelled carrier is sought to be developed and evaluated. It would lead to reduction of pollutant emission as well as reduce the drudgery on the operator. The SPV assisted sprayer will be operated using suitable electric motor and pump while the carrier on which the SPV operated spraying system is to be mounted will be driven by a diesel engine. The developed sprayer is then to be evaluated under field conditions and wheat crop being selected for doing so. Wheat (*Triticum aestivum* L.) is one of the major staple crop grown in India with Punjab being the second largest producer within the country with a production of about 17.35 million tonnes (Anonymous 2019b). During its growing period, many kinds of pests and diseases affect the crop which if not taken care by spraying/dusting ultimately effects its yield and quality.

Keeping in view the above facts, the present study has been undertaken on “Development and evaluation of a solar photo voltaic assisted sprayer mounted on a self propelled carrier” with the following objectives :

1. To develop a solar photo voltaic (SPV) assisted sprayer mounted on a self propelled carrier.
2. To evaluate the developed sprayer for selected sets of operational parameters.

CHAPTER II

REVIEW OF LITERATURE

A comprehensive review of literature is a vital part of any scientific investigation as it gives an idea about what has been done and what needs to be done. It also gives an insight into the theoretical context as well as the method for meaningful interpretation of the finding. With this aim an effort was made to review some of the relevant studies conducted in the past related to the present day. The review has been divided into following sub sections :

1. Solar energy and its applications in sprayers
2. Laboratory and field evaluation of sprayers

2.1 Solar energy and its application in sprayers

Awulu and Sohotshan (2012) developed and evaluated the performance of a electrically operated knapsack sprayer. This setup helped in regulating air pressure which was problematic in conventional knapsack sprayers. The major components were 12 volts accumulator battery, 12 volts electric water pump, tank, belt, delivery pipe and a sprayer handle containing lance and nozzle. Electric pump used was powered by 12 V, 2.5 A battery (motorcycle type). It was observed that the sprayer had a application rate of 250 l/ha, flow rate of 531 ml and a spray distribution area of 6.75 cm². The laboratory test indicated that decrease in liquid head leads to decrease in flow rate and vice versa. Efficiency of spray decreased with decrease in battery voltage and walking speed influenced the application rate. The sprayer was capable of spraying 250 l/ha in 4.17 hours at a walking speed of 0.7 m/s. This device was not able to operate continuously for more than 2 hours due to decrease in voltage. It advised for carrying extra batteries to the farm for large hectare spraying.

Rao *et al* (2013) modified an existing sprayer by replacing the two stroke petrol engine by a DC motor which was operated by a battery attached to the unit. It was observed that time taken to charge the battery to its full capacity (12V, 7Ah) was 16.67 hours. The fully charged battery could be used to spray about 575 litres of pesticide and can cover approximately 5-6 ha of land. The initial cost of developed system was higher as compared to conventional sprayer.

Patil *et al* (2014) developed a solar operated knapsack sprayer using a solar panel of 37 W to facilitate it to operate on two modes i.e. on battery mode and on direct solar panel mode independently. Weight of panel and weight of sprayer was carried on operator shoulder, which enabled effortless operation. After operating for 5 hours in full solar intensity, the sprayer could run for another 2.5 hours on battery which ultimately provided spraying facility at night. Liquid head influenced rate of flow from sprayer. Sprayer was able to spray liquid at 360 l/ha in 4 hours at a walking speed of 0.7 m/s. Rate of discharge of sprayer was 0.0267 l/s.

Yadav (2015) developed a bullock drawn solar powered high clearance sprayer which can also be used for spraying on tall field crops. The developed sprayer consists of solar PV modules, DC motor, battery, spray tank, pump, wheel, seat, spray boom, nozzle, pressure control device and hoses. The performance of sprayer was conducted with three operating pressure (3, 5 and 7 kg/cm²), three nozzle types (hollow cone, solid cone and flat fan) and two pump capacity (25 l/min and 50 l/min). The performance of the sprayer was evaluated in field and laboratory. Field capacity of the bullock drawn solar powered high clearance sprayer was found to be 0.945 ha/h for cotton crop and 1.012 ha/h for red gram crop. For spraying operation, the sprayer is operated at an average travel speed of 2.7 km/h for cotton and 3.0 km/h for red gram crop. The current produced by the panel was 20.88 Ah and the time required for fully charging the batteries was 9.6 h. The area covered using the fully charged battery was 1.9 ha. The cost of operation of bullock drawn solar powered high clearance sprayer was Rs.121.1/h and it was Rs. 128.14/ha for cotton and Rs. 119.66/ha for redgram crop. Breakeven point and payback period were 123.61 h/annum and 3.6 years.

Swami *et al* (2016) designed and developed a solar PV based sprayer. The sprayer operated both on indirect mode and direct mode. In direct mode, the sprayer was operated using electricity obtained from 100 Wp polycrystalline PV modules mounted on the sprayer and in the indirect mode it was operated using battery which stored electric energy in a deep cycle battery (12 V, 32 Ah). A DC motor pump of 60 W was used in both modes to generate the required operating pressure for spraying the liquid pesticide. Brass nozzles, which required an operating pressure of about 1.5-2 kg/cm² were used to provide a discharge of 900 cm³/min. The capacity of the liquid tank of the sprayer was designed to 50 litres capacity for an uninterrupted operation for 2 hours with two nozzles. Solar radiation data from Jodhpur station showed that the sprayer can be best operated during 9:00 am to 3:00 pm. Performance of the developed solar PV sprayer on manually drawn vehicle was tested in field and found satisfactory to spray pesticide in different arid crops.

Vasisht *et al* (2016) studied the performance of a 20 kWp solar photovoltaic (SPV) system at Indian Institute of Science, Bangalore, India, under different seasons and climatic conditions of Bangalore. Over the previous two years the system was producing an average daily yield of approximately 80 kWh which translates to an annual yield of 28.9 MWh. This main focus was on the evaluation of the performance of SPV systems using the popular grading systems, namely Capacity Utilization Factor (CUF) and Performance Ratio (PR). The CUF of the SPV system was 16.5%, which lies within the range of CUF of well-performing solar plants located in India. Average Performance Ratio (PR) of the SPV system was around 85%, which indicated that the performance of the SPV system was satisfactory. PR of the SPV system was correlated with the behaviour of SPV modules in different seasons, with module temperature (T_{mod}) as the key factor of comparison. In summer, the SPV modules attain maximum efficiency (g_{max}) at

T_{mod} of 45°C, but in winter, it was at 55°C. In summer, for $T_{\text{mod}} > 45^\circ\text{C}$, module efficiency (g) reduces by 0.08% per degree rise in temperature. In monsoon, for $T_{\text{mod}} > 35^\circ\text{C}$, g reduces by 0.04% per degree rise in temperature. In post-monsoon period, for $T_{\text{mod}} > 38^\circ\text{C}$, g reduces by 0.06% per degree rise temperature. However, in winters, the modules attain g_{max} at T_{mod} of 55°C, without much drop in efficiency. This is mainly because of intermittent natural cooling that takes places at the surface of the modules, due to cool breeze and lower ambient temperatures.

Yallappa *et al* (2016) developed a agricultural pesticide sprayer operating on solar energy. It comprised of a solar panel of 20 W capacity, a 12 V DC battery charged by solar panel, a DC motor, a pump to spray the pesticide and a tank to hold the pesticide. The entire unit was portable and operated by one labour. The average discharge rate measured in the laboratory and field were almost similar about 0.023 l/s. The sprayer was evaluated for cotton, green gram and onion in the field. Maintaining the walking speed of the operator about 2.8 km/h and swath width of 0.6 m, the theoretical field capacity of the sprayer was 0.17 ha/h. The effective field capacity was about 0.14 ha/h which corresponds to a coverage of 1 ha/day for 8 hours of operation. It was found to be quite economical and eco-friendly as it uses solar energy.

Poudel *et al* (2017) designed and fabricated a solar powered semi automatic sprayer consisting of a solar panel, two DC motors, a battery, pump, microcontroller, container and zigbee device which was operated using a wireless remote having a range of 30 to 50 meters. The container had a capacity of 4 liters, which provided an uninterrupted operation for 10 minutes. The vehicle was powered using an on board solar powered battery which lowers down the running cost. The spraying operation could be done by the farmers without human interference thus protecting them from noxious chemicals.

Chandrashekar *et al* (2018) used a photo voltaic (PV) module for push type solar operated sprayer. The push type solar operated sprayer comprises of a PV module of 20 W and two diaphragm type pumps of 0.03 hp each. The system was tested for its performance in terms of variation in nozzle discharge for different operating pressure and height. It was observed that during normal climatic condition the PV module produced power in the range of 7.1 W to 17.29 W from 10:00 am to 4:00 pm in the month of December 2015. The actual and theoretical field capacity of push type solar sprayer were 0.29 ha/h and 0.32 ha/h for field bean crop with forward speed of 0.53 m/s respectively. The cost of operation of solar operated push type low clearance sprayer was found to be Rs.38.5/h. The push type solar sprayer worked efficiently in row crops and vegetable crops by adjusting swath width as well as height of boom depending upon requirement.

Kingra (2018) attempted to estimate solar radiation from CROPWAT model and then developed regression equations for estimation of solar radiation directly from sunshine hours. Firstly, solar radiation for Ludhiana district was computed from different weather parameters using CROPWAT model and then linear regression models were developed to estimate daily

average solar radiation directly from sunshine hours data on monthly and annual basis. The analysis indicated that annual average solar radiation at Ludhiana was $18.4 \text{ MJ m}^{-2} \text{ day}^{-1}$ with mean monthly solar radiation ranging from $11.2 \text{ MJ m}^{-2} \text{ day}^{-1}$ in December to $24.9 \text{ MJ m}^{-2} \text{ day}^{-1}$ during May. Trend analysis of mean annual solar radiation and sunshine hours indicated a decreasing trend ($R^2 = 0.39$ and 0.41 , respectively). Linear regression models were observed to estimate solar radiation in very good agreement with the solar radiation computed from CROPWAT model with $R^2 > 0.98$ for all the months, which indicates that these models can be used very successfully for empirical estimation of solar radiation from sunshine hours during any period of the year under central Punjab conditions.

Sinha *et al* (2018) considered the case of marginal farmers who preferred knapsack sprayers due to its affordability. They developed a solar powered sprayer which had higher output (0.3 ha/h) with lower physiological energy consumption and discomfort. An electronic control was embedded for protection against deep discharge and over charging of battery for longer operational life. The system was fully charged by solar energy within two hours of irradiation and could be operated continuously for six hours. This ensures good quality of spray with uniform droplet size in the swath. Anti-clogging filter was also installed before the nozzle in nozzle head for trouble free operation as well as longer service life of nozzle. The mean heart rate and Body Posture Discomfort Score (BPDS) were lowest for solar sprayer and covered more than twice (3000 m^2) the area compared to manual and air assisted sprayers indicating lower physiological demand and discomfort to body parts.

Zilpilwar *et al* (2018) developed a solar cum hand operated hybrid knapsack sprayer. Actual field capacity, field efficiency and cost of operation per hour were 0.275 , 86.38% and Rs. 92.63 . The cost of developed sprayer was Rs. 5320 . The farmer could save 1.32 times money using this sprayer compared to hand operated knapsack sprayer.

Mishra *et al* (2019) used a photo voltaic (PV) panel of 6 V , 5 W capacity to perform spraying operation. Solar PV panel was used for operating the sprayer as well as for charging a battery. The motor was used to regulate spraying liquid from the sprayer tank (5 litres) and spray it through spinning disc nozzle. The SPV operated sprayer was provided with a 6 V , 4.5 A lead acid battery which was used as alternate power source during cloudy days (in rainy season).

2.2 Laboratory and field evaluation of sprayers

Mathew *et al* (1992) studied the performance of a power tiller operated boom sprayer. Experiments were performed using hollow cone nozzle under varying pressures. More even distribution was observed at 3 kg/cm^2 compared to that of 2 kg/cm^2 . It was also observed that the cost of operation of boom sprayer reduced by 29% as compared to hand compression knapsack sprayer.

Singh (1996) studied the spray pattern of different types of nozzles i.e. solid cone, hollow cone, adjustable and fan type. It was inferred that on changing the angular setting of the nozzle, there was variation in uniformity of spray distribution pattern and working width of all nozzle. Discharge rate of adjustable and fan type nozzle significantly high compared to hollow cone and solid cone. Hollow cone nozzle was more effective than fan type and solid cone nozzles for spraying pesticides.

Ejaz *et al* (2004) studied the performance of a self-levelling boom sprayer. Self-levelling boom sprayer was tested at 250, 300 and 350 kPa pump pressure against different heights of cotton crop. They inferred that discharge of a nozzle was a function of pressure, shape, size and design. Pressure had significant effect on swath width, spray angle, spray distribution, droplet size and discharge. Along the boom, variation in discharge and spray angle was less at nozzle pressure of 350 kPa as compared to 250 and 300 kPa.

Garg (2004) designed and developed a light weight self propelled boom sprayer. The system was powered by a 3.75 kW diesel engine. The speed of operation was maintained at 2.5-3 km/h. The sprayer covered a swath width of 630-700 mm. The fuel consumption, application rate, field capacity and field efficiency of the sprayer were 0.5-0.6 l/h, 100-120 l/ha, 0.7-0.8 ha/h and 55-60% respectively. The sprayer saved about 80% of labour requirement.

Singh *et al* (2006) conducted studies on the performance of triple action, bi-action and hollow cone nozzles. The experiment was performed at different pressures, heights and nozzle spacings in which pressures were 2.5, 3.0, 3.5 and 4.0 kg/cm², heights were 45, 50 and 60 cm whereas nozzle spacings were 40, 45 and 50 cm. It was inferred that better spray distribution was obtained using bi-action and triple action nozzles as compared to hollow cone nozzle for all the four pressures. The bi-action nozzle produced best results at 3.5 kg/cm² pressure with least coefficient of variation.

Padmanathan and Kathirvel (2007) developed a power tiller operated rear mounted boom sprayer for spraying in cotton and other crops planted in rows. The spray boom had sixteen hollow cone nozzles, placed 40 cm apart. The machine covered a swath width of 3.2 m at a forward speed of 2 km/h. The effective field capacity of the sprayer was 0.72 ha/h. The performance of the power tiller operated boom sprayer was found to be satisfactory at a pressure of 3 kg/cm² and could be adopted by the farmers for spraying cotton crop and other row crops.

Hassan and Bushra (2010) studied the effect of spray application pressure (2 and 4 bars) and forward speed (5.4, 7.9 and 10.8 km/h) on droplet number and volume distribution of spray. All treatments were applied using one nozzle size at one rate of spray application. Average droplet density per cm² increased by 52 % on increasing the pressure from 2 to 4 bars. Increase in the forward speed from 5.4 to 7.9 km/h increased the droplet density by 18.28 %. Increase in forward speed from 7.9 to 10.8 km/h also increased the droplet density by 38.2 %. At pressure 2 bars with forward speed of 10.8 km/h, highest percentage (39 %) of droplet size (30-100 µm)

was obtained, which was in favour of controlling insects. For all levels of speed, higher pressure showed higher uniformity of distribution of spray droplets and lower volume median diameter (VMD) and lower number median diameter (NMD) values. The uniformity coefficient (UC) ratio VMD/NMD was 1.77.

Singh *et al* (2010) developed and evaluated a tractor mounted air-assisted sprayer for spraying on cotton crop and compared with tractor mounted conventional sprayer. The air assisted system of the sprayer consisted of an axial flow fan, fan casing and sleeves with 40 mm diameter holes at 80 mm apart. Droplet size, uniformity coefficient, droplet density, percent area covered by droplet per cm² and bio-efficacy was studied. At a forward speed of 4.0 km/h, better uniformity coefficient (UC) of 1.69 was obtained for the air-assisted sprayer as compared to the conventional sprayer (2.04). Also droplet deposition on the underside of the leaves with the tractor-mounted air assisted sprayer, was in the range of 14 to 94 drops/cm² at different portions of the plant at that forward speed. The area covered by droplets on the underside of top, middle and bottom leaves were 1.11, 0.93 and 0.44% respectively for air-assisted sprayer but there was no droplet deposition by the conventional sprayer. Reduction in the number of whitefly adults was about 30 to 70 % more for tractor mounted air-assisted sprayer than that of tractor mounted conventional sprayer.

Gupta *et al* (2011) studied the consequences of leaf area density, air velocity, nozzle pressure and forward speed on deposition characteristics of an air assisted spraying system on a simulated crop canopy. Droplet size and droplet density on upper side of the canopy were more than that on the under side. Droplet density increased with increase in air speed. Droplet density decreased with increase in leaf area density and forward speed. Leaf area density and forward speed did not influence the droplet size.

Zhu *et al* (2011) developed a portable scanning system that could quickly evaluate spray deposit distribution and coverage area on deposit collectors such as water sensitive paper or Kromekote[®] card. The system is integrated with a handheld business card scanner, deposit collectors, a laptop computer, and a custom-designed software package entitled "DepositScan". The software is composed of a set of custom plug-ins that are used by an image-processing program (ImageJ) to produce a number of measurements suitable for describing spray deposit distribution. The program worked with the handheld business card scanner to scan spray deposits on the collectors. After scanning the collectors, individual droplet sizes, their distributions, total droplet number, droplet density, amount of spray deposits, and percentage of spray coverage are displayed on the computer screen and saved in a spreadsheet.

Hassen *et al* (2013) studied the effect of types of nozzle, angle of spray and pressure on spray volumetric distribution of broadcasting and banding application. Two types of spray nozzles (flat fan nozzle for banding application and standard flat fan nozzle for broadcasting application) was used on the patternator to perform the experiments for determination of spray

pattern. Spray distribution was determined and compared using single nozzle, at a height of 0.5 m under laboratory conditions. The effect of spray fan angles 65 and 80° and liquid pressures 200 and 300 kPa on the spray distribution was also examined. The best distribution of the spray application was obtained by using banding nozzles, whereas the broadcasting nozzle gave an uneven spray distribution with a height just below the nozzle centre and taper off towards the edges of the spray pattern. The results revealed that increasing nozzle angle and pressure reduce the value of the coefficient of variation (CV).

Kalikar *et al* (2013) evaluated the performance of bullock cart mounted engine operated sprayer. The engine of 4 hp was used as power source for operating the sprayer and the bullocks were used for hauling purpose. The sprayer units consist of 9 hollow cone nozzles, adjustable according to row spacing of crop. During performance evaluation, the field capacity of the sprayer was 1.89 ha/h and average speed of bullocks cart during spraying operation in cotton crop was 2.8 km/h. The draft measurement for spraying operation was found to be 804.42 N.

Karale *et al* (2014) developed a self-propelled boom sprayer and evaluated its performance on cotton and chilli. The average effective field capacity of the sprayer in the field of cotton and chilli was 1.28 and 1.69 ha/h with an average field efficiency of 62.74 and 81.02%, respectively. The cost of spraying on using self-propelled sprayer for cotton was about 21% higher than chilli crop.

Anibude *et al* (2016) developed a prototype of animal drawn hydraulic boom sprayer. The main components include spray tank of 100 litres capacity, operator seat, main frame, 3 hp petrol engine, piston pump, boom, ten flat fan nozzles, wheel and axle shaft. The petrol engine powers the piston pump during spraying and pair of bullocks were used for hauling purpose. It was concluded that application rate of 260 l/ha was achieved at an effective field capacity of 1.04 ha/h with a field efficiency of 89.60%.

Jassowal *et al* (2016) evaluated the performance of a tractor operated trailed type boom sprayer under local agro-climatic conditions. The sprayer was operated in the cotton field at three forward speeds (2.5, 3.5 and 4 km/h) and at five fluid flow pressures (3.5, 4.0, 5.0, 6.0 and 7.0 kg/cm²) for its field evaluation. The volume median diameter (VMD) were found to be in the range of 300 – 452 µm. Smaller sized droplets were obtained at higher pressure. The droplet density on leaves varied from 26 to 177 drops/cm². Area covered by droplet spots on upper side of the top leaves, middle leaves and bottom leaves varied from 14.18 to 24.70 mm²/cm², 11.01 to 23.07 mm²/cm² and 8.74 to 17.22 mm²/cm² respectively. Volume of spray deposition on upper side of the top leaves, middle leaves and bottom leaves varied from 330.19 to 677.87 × 10⁻⁶ cc/cm², 293.27 to 633.99 × 10⁻⁶ cc/cm² and 202.71 to 685.57 × 10⁻⁶ cc/cm² respectively. Field capacity of the sprayer was 4.23 ha/h at the forward speed of 4.0 km/h and the average fuel consumption was 4.88 l/h.

Singh (2018) developed and evaluated a multi-nozzle backpack type power sprayer, used for spraying at all stages of cotton crop by using the boom horizontally as well as vertically. Three types of hollow cone nozzles N1, N2 and N3 were evaluated using patternator in the laboratory at pressures of 3.0 kg/cm², 4.5 kg/cm² and 6.0 kg/cm² and at target distances 250 mm, 340 mm and 540 mm respectively. Depending upon laboratory results, nozzle N1 and nozzle N2 were selected for mounting on the boom and operated at a pressure of 3.0 kg/cm² at different target distances. Field capacity of nozzle N2 and N1 decreased from 0.28 ha/h to 0.09 ha/h and 0.34 ha/h to 0.09 ha/h whereas fuel consumption for spraying using the same nozzles increased from 0.37 l/h to 0.50 l/h and 0.42 l/h to 0.60 l/h when the orientation of boom was changed from or horizontal to vertical.

Wang *et al* (2019) compared the droplet deposition, control efficacy and working efficiency of a six-rotor UAV with a self-propelled boom sprayer and two conventional knapsack sprayers on the wheat crop. Water Sensitive Papers (WSP) were used to evaluate the characteristic of deposition such as an area of coverage, number of spray deposits and droplet size. The WSP were fixed horizontally on plastic rods through double-headed clamps. DepositScan, an imagery software was used to extract droplet deposits in the digital image and analyze the droplet size, number of spray deposits and the area of coverage. The total deposition of UAV and other sprayers were not statistically significant, but significantly lower for run-off. The deposition uniformity and droplets penetrability of the UAV were poor. The deposition variation coefficient of the UAV was 87.2%, which was higher than the boom sprayer of 31.20%. The deposition on the third top leaf was only 50.0% compared to the boom sprayer. The area of coverage of the UAV was 2.2% under the spray volume of 10 L/ha. The control efficacy on wheat aphids of UAV was 70.90%, which was comparable to other sprayers. The working efficiency of UAV was 4.11 ha/h, which was roughly 1.7–20.0 times higher than the three other sprayers. Comparable control efficacy results suggest that UAV application could be a viable strategy to control pests with higher efficiency. Further improvement on deposition uniformity and penetrability are needed.

CHAPTER III

MATERIAL AND METHODS

This chapter deals with the methods and materials used in this study. The overall procedure has been described under the following heads.

1. Development of the solar photovoltaic assisted sprayer.
2. Development of the self propelled carrier for mounting the spraying assembly.
3. Performance evaluation of the solar photovoltaic operated sprayer mounted on a self-propelled carrier.
4. Statistical analysis.

3.1 Development of the solar photovoltaic assisted sprayer

3.1.1 Solar power potential

India is endowed with vast solar energy potential. About 5,000 trillion kWh per year energy is incident over India's land area with most parts receiving 4-7 kWh per sq. m per day. The Global Horizontal Irradiation (GHI) at various regions of India (Anonymous 2019c) is shown in Fig 3.1.

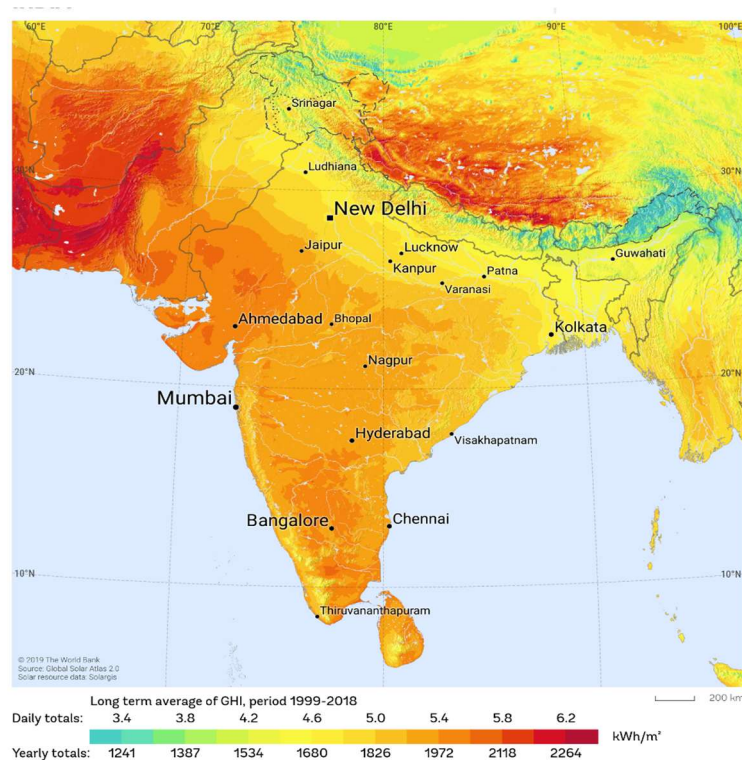


Fig 3.1: Map showing global horizontal irradiation in India

3.1.2 Selection of motor

Based on the availability, a 12 V 3.0 A dual diaphragm type pump-motor combo was selected for performing the necessary operation as shown in Fig 3.2. This pump-motor combo is electrically operated and can be driven using batteries or solar power source. The specifications of the pump-motor combo is shown in Table 3.1.

Table 3.1: Specifications of diaphragm pump motor

Voltage	12 V, DC
Maximum Current	3.0 A
Maximum Pressure	6.628 kg/cm ²
Open Flow	4.0 l/min



Fig 3.2: Diaphragm pump motor

3.1.3 Selection of battery

Batteries are an important component for storage and supply of DC power. The requirement and selection of the batteries was based on the power required to run the diaphragm pump-motor operating the sprayer. Theoretical calculation of power required by the motor is as follows:

Based on the selected diaphragm pump motor, for each motor,

$$\text{Maximum voltage (V)} = 12 \text{ V}$$

$$\text{Maximum current (I)} = 3 \text{ A}$$

As there are two numbers of pump motor, therefore, the maximum power (P) required to run the motor :

$$P = 2 \times V \times I \quad (3.1)$$

$$= 2 \times 12 \times 3 = 72 \text{ W}$$

Now, considering that the sprayer needs to be run for 8 hours in a day, the total energy (E) required to be supplied is :

$$E = P \times \text{No. of hours of operation}$$

$$= 72 \times 8 = 576 \text{ Wh}$$

The most commonly available and cost effective type of battery available in the market is the lead acid battery. As the diaphragm pump motor is rated at 12 V, a lead acid battery of 12 V is to be selected. Considering the lead acid battery has a depth of discharge of 75%, the theoretical maximum capacity (C) of the battery therefore required is :

$$C = \frac{E}{\text{Battery voltage} \times 0.75} \quad (3.2)$$

$$= \frac{576}{12 \times 0.75} = 64 \text{ Ah}$$

3.1.4 Selection of the solar PV panels

Photo-voltaic cells use energy from sunlight (photons) and generate direct current electricity through photovoltaic effect. An assembly of PV cells is called a PV module while a collection of PV modules is called a PV panel. A PV junction box is attached to the back of the solar panel and functions as its output interface. The selection of solar panels was based on the power requirement to fully charge the battery required to run the sprayer so that the operator can continuously operate the sprayer the next day without any further external charging. Calculation for requirement of solar panels is as follows :

As discussed in section 3.1.3, lead acid battery of 12 V 64 Ah capacity is required to run the pump motor required for spraying operation. Hence, the total energy (T) required to be supplied using solar panels:

$$\text{Total energy (Wh)} = 12 \times 64 = 768 \text{ Wh}$$

The average number of sunshine hours during winters in Ludhiana, Punjab was 7.48 hours as estimated by (Kingra 2018). Hence, required power of solar panel (P_L) required:

$$\text{Power of panel required (P}_L) = \frac{768}{7.48} = 102.67 \text{ W}$$

A solar panel of 102.67 W will be able to generate the required power only when radiation is incident on the solar panel at 1000 W/m² i.e. at Standard Test Conditions (STC). In winter season (November to March), the average solar radiation in district Ludhiana, Punjab is about 528.07 W/m² (Kingra 2018). Hence, the actual approximate rated power of solar panel (P_V) can be calculated using the follow equation (Chilundo *et al* 2018):

$$P_V = \frac{P_L \times G_{REF}}{G_{Glob} \times F_Q} \quad (3.3)$$

where,

G_{REF} = Incident solar radiation at STC (1000 W/m²)

G_{Glob} = Global solar radiation on a horizontal surface (W/m²)

F_Q = Quality factor of the system = 0.8 for PV array

$$\begin{aligned} P_V &= \frac{102.67 \times 1000}{528.07 \times 0.8} \\ &= 243 \text{ W} \end{aligned}$$

Hence, theoretically solar panels of 243 Wp is required to fully charge lead acid battery of 12 V 64 Ah capacity on a typical working day in winter season .

3.1.5 Selection of solar charge controller

The solar charge controller's primary function is to maintain the amount of charge coming from the solar PV module that flows into the battery bank in order to avoid the batteries being overcharged. It limits and regulates the voltage from the solar panel to avoid overcharging the battery. While DC loads are being used, the controller does not allow the battery to get discharged (Majaw *et al* 2018). Hence, a cost effective PWM (Pulse Width Modulation) type solar charge controller of "amiciSmart" make, able to withstand 12/24 V, 40 A shown in Fig 3.3 was selected for development of solar PV assisted sprayer. The controller regulates the incoming voltage from the panel according to the requirement of the battery. The solar charge controller contains a display panel which shows the voltage and the current generated by the solar panels. It also shows the voltage and current during discharge by the diaphragm pump motor as well as the voltage of the battery. The charge controller also has a provision for displaying the ambient temperature. It also contains two USB ports.



Fig 3.3: Solar charge controller

3.1.6 Selection of the nozzles

For the solar PV assisted sprayer, the selection of the nozzles were based on the discharge capacity and pressure generated by the pump motor combo. Hence, hollow cone nozzles (TXA800050VK) of TeeJet Technologies were selected for development of the sprayer, shown in Fig 3.4. Hollow cone nozzles can generally be used to apply insecticides or fungicides to field crop where plant foliage penetration and complete coverage of leaf surfaces is essential (Singh 2017).



Fig 3.4: Hollow cone nozzle

3.1.6.1 Study of the nozzle characteristics

Selected nozzle was evaluated in the laboratory as per levels of independent variables given in Table 3.2, using patternator available in the Farm Machinery Testing Centre, Department of FM&PE, COAE&T, PAU, Ludhiana. The study of the nozzle characteristics helped in determining the optimum pressure and height to be taken for evaluating the developed sprayer in field.

Table 3.2: Levels of independent and dependent parameters used for laboratory study

Independent variables	Levels	Remarks	Dependent variables
Pressure	3	2,3 and 4 kg/cm ²	<ul style="list-style-type: none">● Discharge rate● Spray angle● Swath width● Spray distribution pattern
Height	3	45,50 and 55 cm	

3.1.6.1.1 Patternator

A 2×2 m spray patternator having 63 rectangular channels of acrylic sheet with inner dimension of each channel equal to 200×3×10 cm (Length × Width × Height) was used for study, shown in Fig 3.5. Volume of liquid at different nozzle settings was collected in tubes and measured at different nozzle pressure, and nozzle height on spray pattern. The inclination of the spray channel section was adjustable. The nozzle holding arrangement has been made at the top in the middle of the main frame. There is a provision to increase or decrease the distance between the nozzles and surface of the patternator. The sheets were inclined at 9-10° angle. The whole setup consisted of multistage pump, pressure gauge, throttling valve and plastic container for water collection.



Fig 3.5: Spray patternator

3.1.6.1.2 Discharge rate

When the pressure of liquid flowing through nozzle gets stabilized, the discharge of liquid from the nozzle is collected for one minute in the measuring glass. The average volume of collected liquid at each pressure was the discharge rate (per minute basis) at that pressure.

3.1.6.1.3 Spray angle

The angle made by the liquid coming out of the nozzle at each operating pressure was recorded as spray angle at that pressure. The spray angle was measured using a protractor.

3.1.6.1.4 Swath width

The average width of liquid sprayed by the nozzle at each pressure and height above the patternator into different channels was termed as swath width at that pressure and height of the nozzle.

3.1.6.1.5 Spray distribution pattern

A single nozzle was mounted on the top at central position of the patternator. The liquid sprayed in one minute was collected from each channel of the patternator in the glass tubes and volume of liquid collected in each tube was recorded. The average values of the volume of collected liquid from the channels were used to determine spray distribution pattern.

3.1.6.2 Nozzle Spacing

The overlapping of spray pattern of single nozzle was done on MS Excel at different pressures and height. The minimum coefficient of variation (CV) of overlapped pattern was used to select the spacing of nozzles to be mounted on a boom.

3.1.7 Initial testing of the solar PV assisted sprayer

The developed sprayer was operated at a pressure of 3 kg/cm² as selected from laboratory evaluation taking 8 number of nozzles and using a battery as shown in Fig 3.6. The sprayer was operated continuously for 8 hours and it was observed that the maximum current drawn by the pump motor during the day was 3.5 A and hence, the required spraying operation can be completed using 12 V 26 Ah battery shown in Fig 3.7.



Fig 3.6: Initial testing of the spray boom using battery



Fig 3.7: Lead acid battery

For the given battery configuration, the actual rated power of solar panel required can be calculated using the procedure as discussed in section 3.1.4. Hence, the total energy (T) required to be supplied using solar panels:

$$\text{Total energy (Wh)} = 12 \times 26 = 312 \text{ Wh}$$

Average number of sunshine hours during winters in Ludhiana, Punjab = 7.48 hours

Hence, required power of solar panel (P_L) required:

$$P_L = \frac{312}{7.48} = 41.71 \text{ W}$$

A solar panel of 41.71 W will be able to generate the required power at Standard Test Conditions (STC) only.

Average solar radiation in Ludhiana, Punjab during winter season = 528.07 W/m²

Hence, the actual approximate rated power of solar panel (P_V) can be calculated using the following equation :

$$P_V = \frac{P_L \times G_{REF}}{G_{Glob} \times F_Q} = \frac{41.71 \times 1000}{528.07 \times 0.8} = 98.73 \text{ W}$$

Hence, solar panel of 98.73 Wp is required to charge the battery. As solar panel of 100 Wp was commercially available, a polycrystalline solar panel of “Green Solar” make was selected for mounting on the sprayer shown in Fig 3.8. The specifications of the solar panel is shown in Table 3.3. The surface area of the solar panel was 0.64 m². Additional space has been provided on the frame for mounting another panel when the solar radiation is low.



Fig 3.8: Solar panel

Table 3.3: Specifications of solar panel

Power (P_{max})	100 W
Open circuit voltage (V_{oc})	22.0 V
Short circuit current (I_{sc})	6.0 A
Current at maximum power (I_{pm})	5.56 A
Voltage at maximum power (V_{pm})	18.0 V

3.1.8 Assembly of parts for solar PV assisted sprayer

As described above, the major parts of the solar PV assisted spraying assembly consists of solar panels, battery, solar charge controller, boom containing nozzles and spray tank. A cylindrical shaped spray tank of 100 litres capacity was installed so that it can contain sufficient spray mixture to operate for sufficient time and cover a large area in one filling of the tank. Plastic hose pipes of 12 mm diameter were used to carry the spray mixture from the tank to the pump-motor as well as supply the mixture from the pump-motor to the nozzles on the boom. A gate valve is provided in the hose pipe between the pump-motor and the spray boom to regulate the pressure of the fluid flowing to the nozzles as well as bypass the excess fluid back to the spray tank. A pressure gauge adapter containing a pressure gauge is mounted above the nozzle to read the pressure of the fluid in the nozzle. A complete circuit diagram of the solar PV assisted spraying system is shown in Fig 3.9.

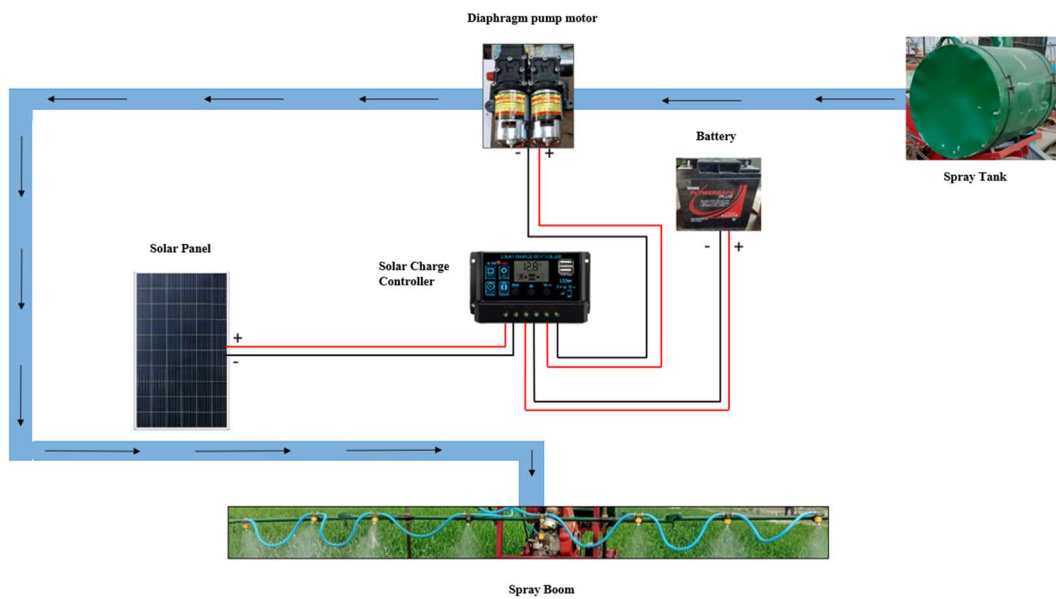


Fig 3.9: Circuit diagram of the SPV assisted spraying system

3.2 Development of the self-propelled carrier for mounting the spraying assembly

The development of the self-propelled carrier for mounting the spraying assembly was done at the Prototype Production Centre, Department of FM&PE, COAE&T, PAU, Ludhiana. A three wheeled frame available at the Research Hall, Department of FM&PE, as shown in Fig 3.10 was selected for mounting the solar operated spraying system.



Fig 3.10: View of the available frame

As the carrier is to be a self propelled type, so a 5 hp diesel engine was used for delivering the power to drive the carrier. The specifications of the diesel engine is shown in Table 3.4.

Table 3.4: Specifications of the diesel engine

Make	Greaves
Model	5520
Brake horse power	5 hp
RPM	3600
Specific fuel consumption	220 g/bhp-h

The two front wheels of the carrier are the powered wheels while the third wheel is free to drive and rotate to take turns. Power and required drive to the front wheels was delivered using belt-pulley and chain-sprocket sets. The drive from the engine goes through a smaller driving pulley to a larger driven pulley using a V-belt and from the larger pulley the power and the drive goes to the wheels through chain and sprockets. The speed of the engine was controlled using a throttling lever. A lever is provided for connecting and disconnecting the drive from the driven pulley to the chain sprocket assembly. Clutch levers are provided on both sides of the handle which are further connected to the wheels for connecting and disconnecting the drive while taking turns. At the front of the carrier is a rectangular frame for mounting the tank. In front of this rectangular frame is a flat plate for mounting the diaphragm pump motor. Below the rectangular frame is a L-shaped attachment made of iron flats having a bracket mounted on it which holds the battery.

At the rear end of the three wheeled frame, a U-shaped frame made of square bars was attached. On top of this frame, another frame made of angle iron bars was attached for mounting the solar panels as well as the spray boom on the rear side. The frame for mounting the solar panels was oriented parallel to the ground so as to harness maximum amount of solar energy as well as maintain stability while operating in field. The height of this frame was selected considering the operator can stand freely while operating. Also, the width of this frame had been so selected so that the operator has enough space for walking and operating the sprayer without any difficulty. Two hollow iron pipes were connected at the back of the frame for mounting the spray boom. Provision for changing the height of boom along the hollow iron pipes has also been provided. Flat iron bars are provided on both sides of the frame to maintain strength and rigidity of the frame as well as the boom.

The resulting machine is a walk behind type of machine where the operator is only needed to operate the given controls and to control the direction of the machine while moving

in the field. The track width and wheel base of the solar operated sprayer mounted on a self propelled carrier are 90 cm and 105.80 cm respectively. The maximum height of the machine from the ground is 206.40 cm. Ground clearance of the machine is 52 cm. The overall length of the machine is 270 cm. The conceptual 3D drawing (Fig 3.11) of the machine was made using Solid Edge V20 while the 2D drawings (Fig 3.12) of the machine showing all the labels and dimensions (in mm) were drawn using AutoCAD 2018. The actual view of the machine is shown in the Fig 3.13.

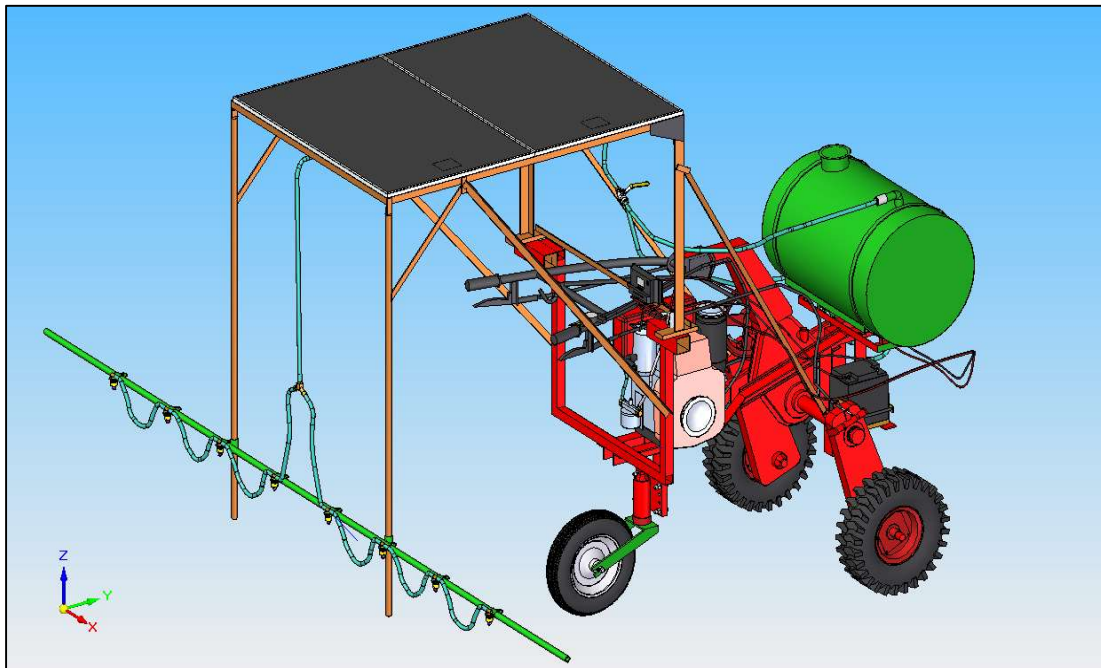


Fig 3.11: 3D view of the machine

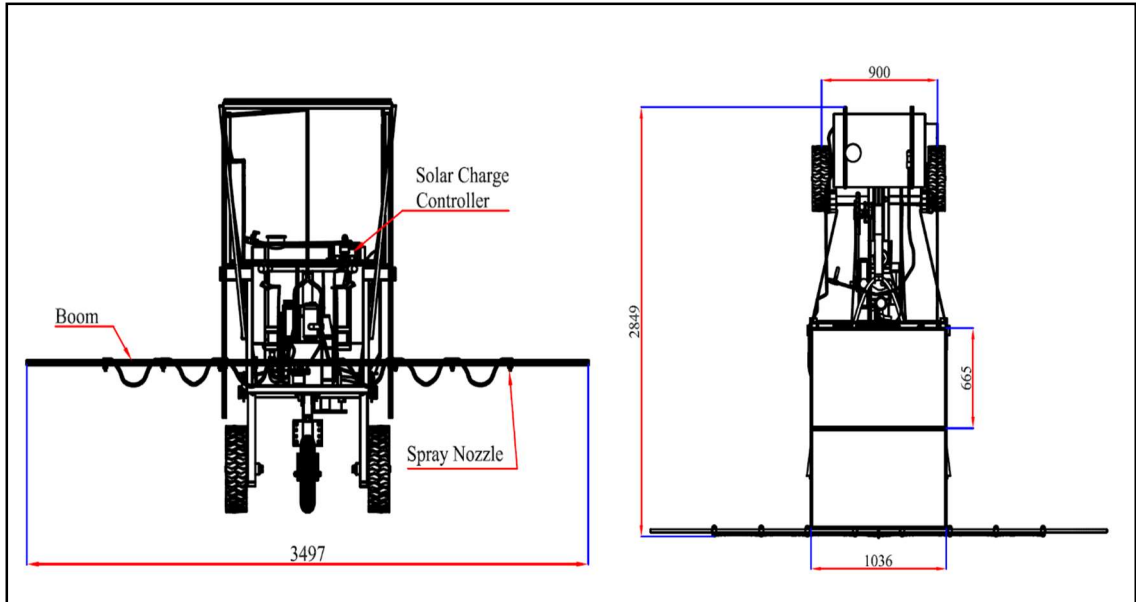
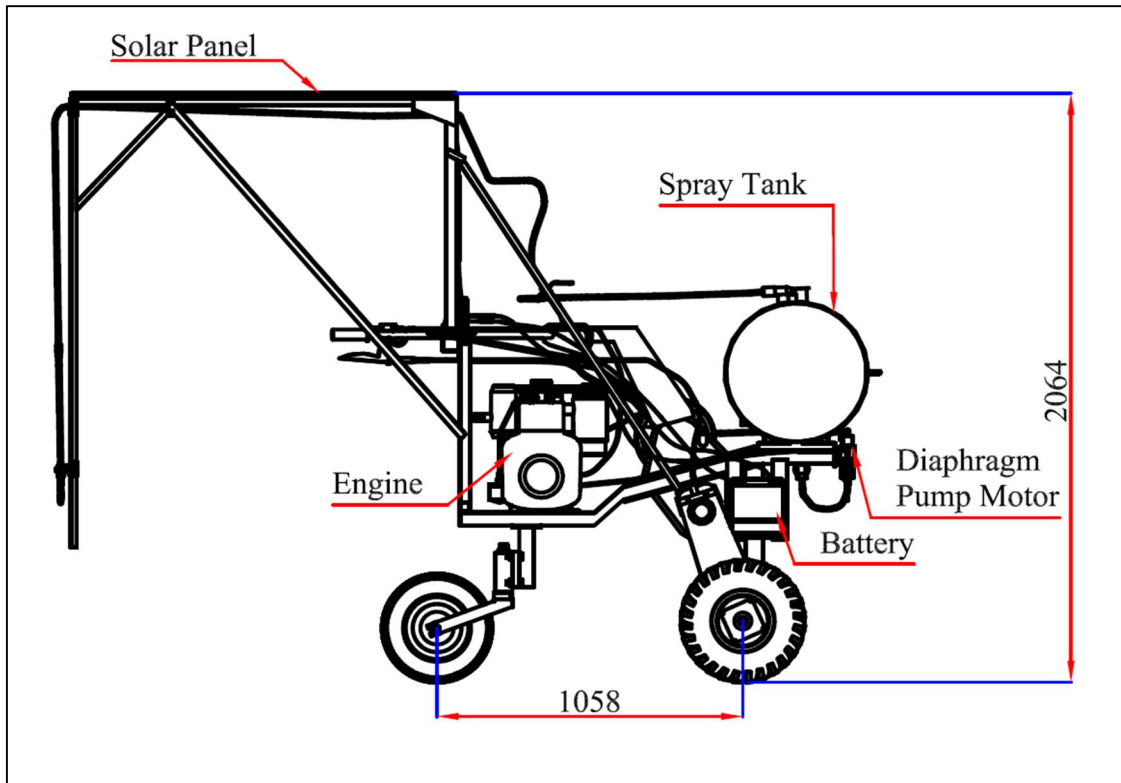


Fig 3.12: 2D conceptual views of the machine



Fig 3.13: Actual view of the developed machine

3.3 Performance evaluation of the solar photovoltaic assisted sprayer mounted on a self propelled carrier

The developed sprayer was evaluated under field conditions. Wheat crop was selected for performing the spraying operation. All field experiments/evaluation of the sprayer was carried out at the research farm of Department of FM&PE, COAE&T, PAU, Ludhiana. Late variety wheat PBW-550 was sown on 4th December, 2020 and spraying operation was performed when average height of the crop reached 40-45 cm. Row to row spacing of the wheat crop was 22 cm.

Firstly this sprayer was evaluated for studying its performance throughout a typical day in January, 2021. Then field evaluation was carried out on wheat crop to study the spray characteristics and field parameters.

3.3.1 Performance evaluation of the solar PV setup

On a typical day, while operating the SPV assisted sprayer, observations of the voltage, current, incoming solar radiation on the panel surface, ambient temperature, panel temperature were recorded after every half hour duration from 9 am to 5 pm (Fig 3.14). Charging voltage and current was recorded from the solar charge controller itself by reading the data on the display panel. The incoming solar radiation incident on the panel surface was recorded by placing a solar power meter on the panel surface. The panel temperature was recorded using an infrared thermometer. The instruments used for recording the observations are shown in the Fig 3.15 and 3.16.



Fig 3.14: Recording of panel temperature and solar radiation



Fig 3.15: Solar power meter

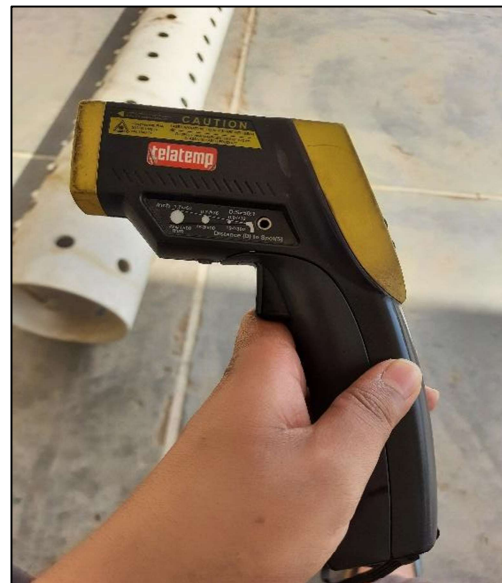


Fig 3.16: Infrared thermometer

The recorded observations were used to study the performance of the solar panels and the following parameters were studied:

3.3.1.1 Array output

It refers to the power (watts) generated by the solar panels at their output terminals due to the incident solar radiation on the panel surface. It is given as:

$$\text{Array output (W)} = V \times I \quad (3.4)$$

where, V = DC voltage, V

I = DC current, A

3.3.1.2 Efficiency of PV panel or conversion efficiency

Efficiency of a PV panel or conversion efficiency denotes the ability of a PV panel to generate output electrical power from the incident solar radiation falling on the panel surface. It can be defined as the ratio of the energy output to the energy input from the sun (Patil *et al* 2014).

$$\text{PV Efficiency (\%)} = \frac{\text{Output Power (W)}}{\text{Input Power (W)}} \times 100 \quad (3.5)$$

$$= \frac{\text{Voltage produced (V)} \times \text{Current developed (A)}}{\text{Incident solar intensity } \left(\frac{\text{W}}{\text{m}^2}\right) \times \text{Area of the array (m}^2\text{)}} \times 100 \quad (3.6)$$

3.3.2 Field evaluation of the SPV assisted sprayer mounted on a self propelled carrier

The developed SPV assisted sprayer was evaluated under field conditions on wheat crop to study the field and spray parameters. The field experiments were carried out at Research Farm, Department of FM&PE, COAE&T, PAU, Ludhiana, shown in Fig 3.17. The machine was operated at two different forward speeds (0.6 and 0.7 m/s) and field measurements were taken at respective speeds. As it is a walk behind type self propelled machine, the forward speeds were selected considering average walking speed of a human. The forward speeds can be adjusted using the throttling lever. Forward speeds were selected by marking two poles at 20 m distance apart and noting down the time taken by the machine to cover that distance and subsequently calculating the forward speed. The levels of independent and dependent parameters used for field evaluation of the sprayer is shown in Table 3.5.

Table 3.5: Levels of independent and dependent parameters used for field evaluation

Field Parameters			
Independent variables	Levels	Remarks	Dependent variables
Forward speed	2	0.6 and 0.7 m/s	<ul style="list-style-type: none"> ● Swath width ● Application rate ● Field capacity ● Field efficiency
Number of nozzles	3	4, 6 and 8	
Spray Parameters			
Independent variables	Levels	Remarks	Dependent variables
Pressure	3	2, 3 and 4 kg/cm ²	<ul style="list-style-type: none"> ● Droplet size <ul style="list-style-type: none"> ● Number median diameter (NMD) ● Volume median diameter (VMD) ● Uniformity Coefficient (UC) ● Droplet deposition <ul style="list-style-type: none"> ● Droplet density ● % Spray coverage area ● Ground losses
Forward speed	2	0.6 and 0.7 m/s	



Fig 3.17: Field operation of the solar photovoltaic assisted sprayer mounted on a self propelled carrier

3.3.2.1 Field parameters

3.3.2.1.1 Swath width

Swath width as described here is the total width of spray of the boom containing nozzles. The swath width was measured by operating the machine on a open plain field for a length of 20 m. Then visualizing the spray pattern, the swath width was measured using a measuring tape.

3.3.2.1.2 Application rate

Application rate can be defined as the total amount of spray material applied per unit area. It can be determined by the following formula (Sharma and Jain 2019) :

$$\text{Application rate (l/ha)} = \frac{60000 \times Q}{S \times W} \quad (3.7)$$

where,

Q = Total discharge from all the nozzles of the boom, l/min

S = Forward speed, km/h

W = Swath width, cm

3.3.2.1.3 Field capacity

Theoretical field capacity is the rate of field coverage if the developed sprayer operates continuously without interruption. It can be calculated by the formula (Kepner *et al* 1987) :

$$\text{Theoretical field capacity (ha/h)} = \frac{W \times S}{10} \quad (3.8)$$

where,

W = Swath width, m

S = Forward speed, km/h

Actual field capacity is the actual rate of field coverage based on actual spraying time. This was calculated by measuring the area covered and dividing by the actual time taken. The actual time consisted of time taken for spraying, turning, filling up of tank and time required to travel to water filling point. The actual field capacity was determined using following formula (Kepner *et al* 1987) :

$$\text{Actual field capacity (ha/h)} = \frac{A}{T \times 10000} \quad (3.9)$$

where,

A = Area covered by the sprayer, m²

T = Average time taken, h

3.3.2.1.4 Field efficiency

Field efficiency is the ratio of actual field capacity to the theoretical field capacity expressed in percentage. It can be calculated using the formula (Kepner *et al* 1987) :

$$\text{Field efficiency (\%)} = \frac{\text{Actual field capacity}}{\text{Theoretical field capacity}} \times 100 \quad (3.10)$$

3.3.2.2 Spray parameters

The sprayer was evaluated on wheat crop for spray parameters at three different nozzle pressures and height setups of 2 kg/cm² & 55 cm, 3 kg/cm² & 55 cm and 4 kg/cm² & 45 cm as selected from laboratory evaluation for minimum coefficient of variation and at forward speeds of 0.6 and 0.7 m/s. The spray parameters to be determined were characterized as droplet size and droplet deposition.

As the leaves of the wheat crops are very light, they get easily disturbed due to the action of wind and machine movement within the rows of the crop. So, mounting the water sensitive papers onto the leaves of wheat crop is not advantageous and we might get uneven distribution. Hence, stands or replicas similar to wheat crop were made and planted within the crop rows. Similar type of study of using stands to hold water sensitive papers in wheat crop was conducted by (Wang *et al* 2019). Water sensitive papers (2.6 x 7.6 cm) were attached in the upper and underside of the stand at two different heights (Top and Middle) acting as wheat canopy. One water sensitive paper was attached at the bottom of the stand for determination of ground losses. The stand or replica of wheat crop with the water sensitive papers attached is shown in Fig 3.18.

After the spraying experiment had been performed, all the water sensitive papers were collected and placed into Zip-lock bags to prevent them from moisture. The cards were then taken to be analyzed for spray parameters using DepositScan software developed by the USDA.



Fig 3.18: Stands holding water sensitive papers in wheat crop

DepositScan (Fig 3.19) is a scanning program that can quickly evaluate spray deposit distribution on water sensitive paper or Kromekote® cards. The program consists of a set of custom plugins that are used by an image processing program to produce a number of measurements useful for expressing spray deposit distribution. The DepositScan program offers a convenient solution for on the spot evaluation of spray quality even under field working conditions.

The software can be operated using a laptop or a desktop computer. For using the software, firstly the water sensitive papers needs to be scanned using a scanner at 600 dpi resolution. In our case, the water sensitive papers were scanned using “EPSON Expression 12000XL” scanner (Fig 3.20) at 600 dpi resolution available at the Precision Agriculture Laboratory, Department of FM&PE, COAE&T, PAU, Ludhiana. The scanned papers were then processed using the DepositScan software (Fig 3.21) in the following steps :

1. After opening the scanned image in the DepositScan software, the actual dimensions and unit of the water sensitive paper are set using “Set Scale” command under “Analyze” tab.
2. For processing the image, the image is converted to 8-bit form using “Type” command under “Image” tab.
3. After conversion of the image, a best suited and clearly visible 1 cm² area of the image is to be cropped for image analysis.

4. Threshold of the cropped image is then done to adjust the image detection quality. Click on the “T” in the option box, a threshold box will appear entering the threshold to define the image detection quality that matches the actual deposit patterns.
5. After threshold, click on the water paper analysis “AA” in the option box for image analysis. The result sheet will appear. Click “Save” to save the report to a data file, which can be opened by Microsoft Excel.

The saved data file contains values of $D_{V0.1}$, $D_{V0.5}$ and $D_{V0.9}$, and displays the results from the area of the selected section, the total number of spots and the percentage area covered by the spots. $D_{V0.1}$, $D_{V0.5}$, and $D_{V0.9}$ represent the distribution of the droplet diameters such that droplets with a diameter smaller than $D_{V0.1}$, $D_{V0.5}$, and $D_{V0.9}$ compose 10%, 50% and 90% of the total liquid volume, respectively (Zhu *et al* 2011).

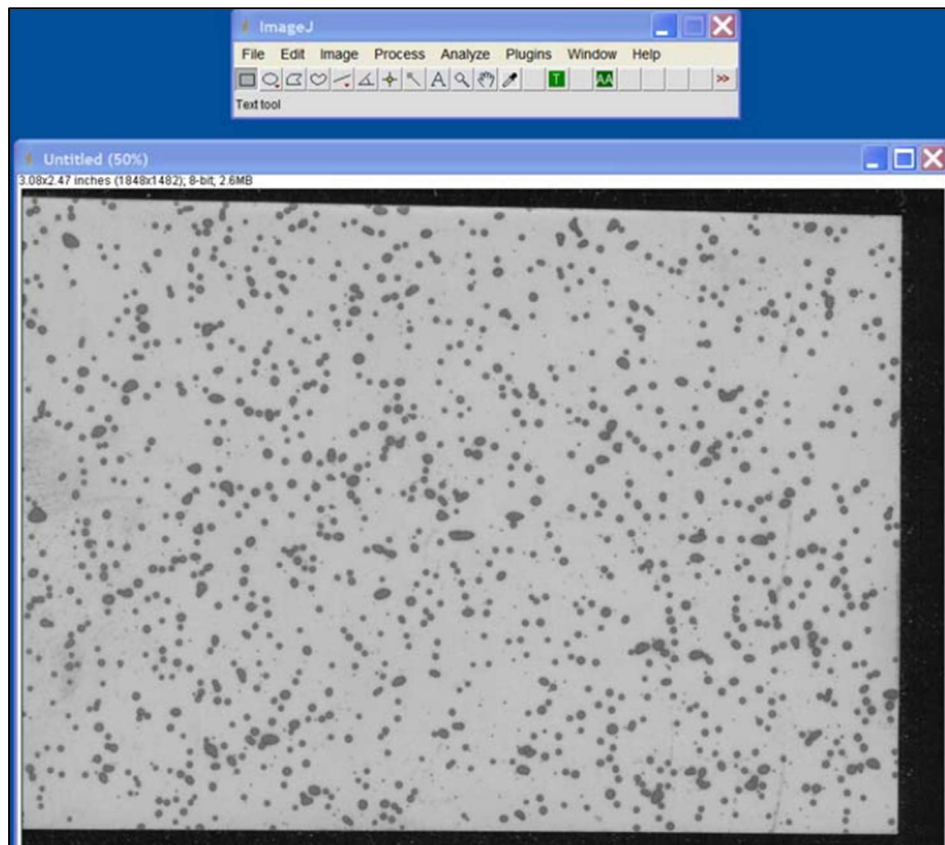


Fig 3.19: Interface of DepositScan software



Fig 3.20: Scanning of water sensitive papers using scanner

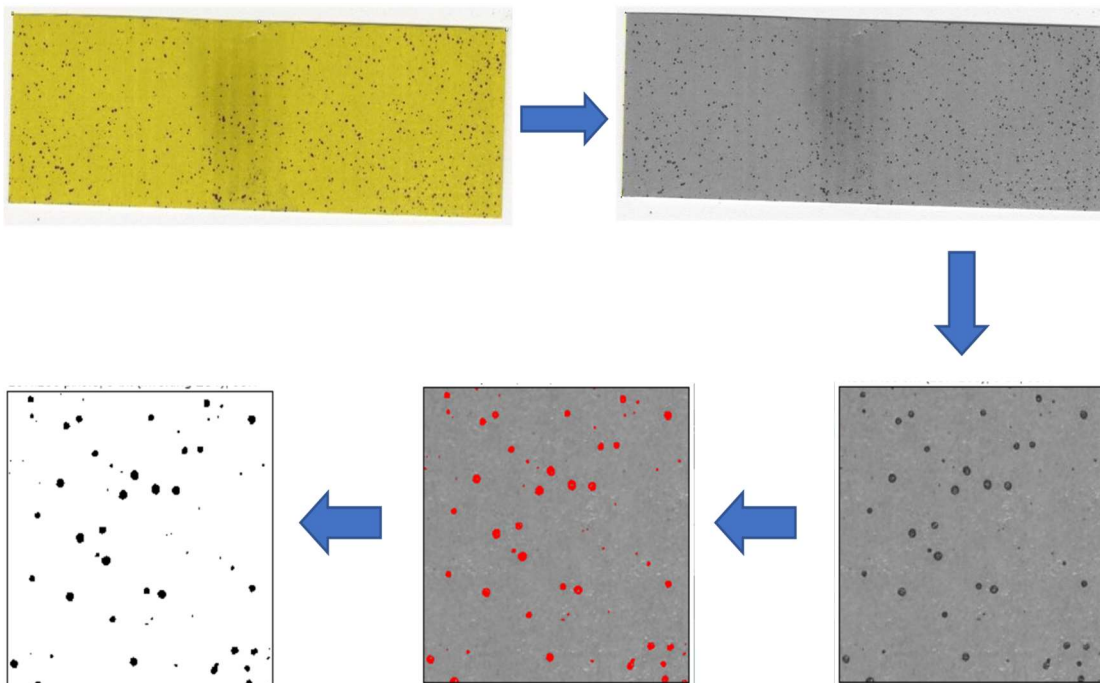


Fig 3.21: Image processing in DepositScan software

3.3.2.2.1 Droplet size

Droplet size is the mean diameter of droplets expressed in microns. The use of small droplets offers potential savings, as the relationship between volumes is directly proportional the third power of droplet diameter. It also have a characteristic of having a lower momentum and would be easily drifted away from the targeted area. Whereas, large droplets have a higher momentum where it could bounce and reflected from the plant surface. Hence, proper selection of droplet size play a significant role to achieve the uniform spray. Most of the spray nozzles produce a wide range of droplets size because of the formation of droplet in randomized process of droplet formation during sheet breakup. The variation in droplet sizes depends on the type of nozzle and its operating pressure. The droplet size can be measured in terms of Volume Median Diameter (VMD) and Number Median Diameter (NMD). Uniformity coefficient can be obtained from division of VMD by NMD. The value of UC should be nearer to 1 to attain a perfect spray pattern.

The DepositScan software uses an equation to convert the spot area to the actual droplet diameter ($d, \mu\text{m}$) which is given as follows :

$$d = 0.95 \times d_s^{0.910} \quad (3.11)$$

where,

$$d_s = \sqrt{\frac{4A}{\pi}}$$

$A = \text{Spot area, } \mu\text{m}^2$

The software calculates the spot area using the number of spot image pixels divided by the scanning resolution.

After all the deposits are converted into actual droplet diameters, the diameters are sorted from smallest to largest, and based on the calculated diameter, The following equation is then used to calculate the volume of each droplet :

$$V_i = \frac{\pi d_i^3}{6}, \quad i = 1, \dots, N \quad (3.12)$$

where,

$V_i = \text{Individual droplet volume, } \mu\text{m}^3$

$d_i = \text{Individual droplet diameter, } \mu\text{m}$

$i = \text{Order of the individual droplet in the sorted range}$

$N = \text{total number of droplets on the sample collector}$

After the volume of each droplet is calculated, the cumulative volume (V_j) and percentage cumulative volume ($\%V_j$) of droplets are calculated using the following equations :

$$V_j = \sum_{i=1}^j V_i, \quad j = 1, \dots, N \quad (3.13)$$

$$\%V_j = \frac{V_j}{V_N} \times 100 \quad (3.14)$$

where,

j = Sequenced order of the droplets in the sorted range

The program then searches for droplet diameters at the point where $\%V_j = 10$ for $D_{V0.1}$, $\%V_j = 50$ for $D_{V0.5}$, and $\%V_j = 90$ for $D_{V0.9}$. $D_{V0.5}$ in the data file represents the volume median diameter (VMD). The number median diameter (NMD) can be found by calculating the median value of all the actual diameters of droplets from the data file. The uniformity coefficient (UC) can then be calculated by dividing the VMD by NMD.

3.3.2.2.2 Droplet deposition

The DepositScan software counts the number of droplets present in the water sensitive paper when image analysis is done taking 1 cm² area. The number of droplets per square centimeter area is defined as droplet density. Droplet density plays an important role with the droplet size from the point of view of quantity and quality of spray. Droplet density also decides the effectiveness of the pest control depending on the operational parameters.

The software also calculates the percentage area coverage by the spray droplets per centimeter square of image area.

Some water sensitive papers were mounted near to the ground surface onto the stands. These papers were analyzed in DepositScan software to calculate the amount of ground losses at different forward speeds and pressures.

3.4 Statistical analysis

Statistical Analysis Software (SAS) was used for conducting analysis of variance to test the significance of each independent variable and their interaction on the dependent variable at 5 percent level of significance. Factorial in Randomized Block Design (FRBD) was used to study the effect of independent parameters on spray parameters at top and middle canopy of wheat crop.

CHAPTER IV

RESULTS AND DISCUSSION

This chapter discusses the development of the solar photovoltaic assisted sprayer mounted on a self propelled carrier. It also presents the results obtained from laboratory and field studies on this developed sprayer and discusses the results.

4.1 Laboratory evaluation of the hollow cone nozzle

4.1.1 Nozzle characteristics

4.1.1.1 Rate of discharge

The hollow cone nozzle was operated at different pressures and its effect on the rate of discharge was observed as shown in Fig 4.1. It was observed that the rate of discharge increased with increase in pressure.

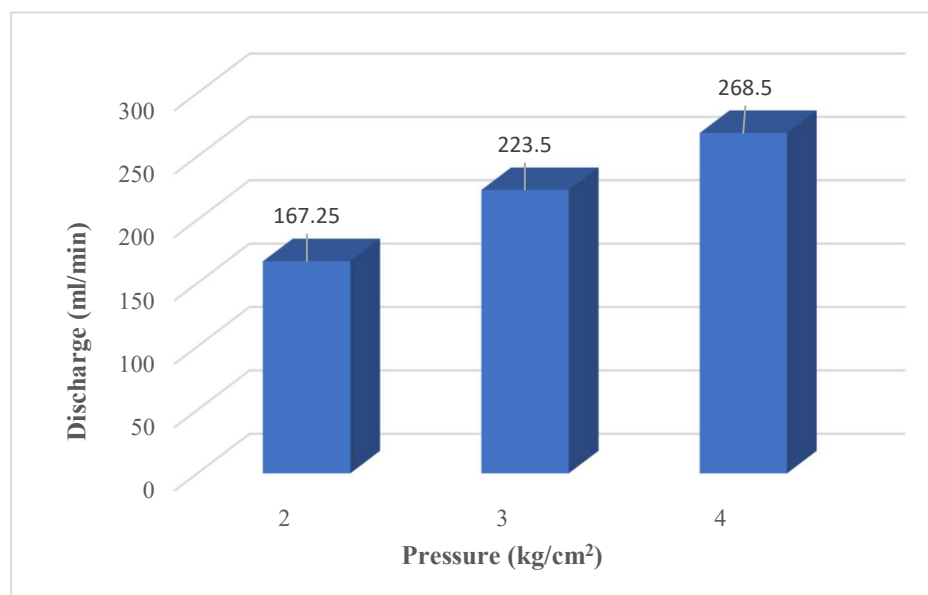


Fig 4.1: Effect of different pressures on discharge

4.1.1.2 Spray angle

The effect of different pressures on the spray angle of the nozzle is shown Fig 4.2. It was observed that the spray angle increased with increase in pressure.

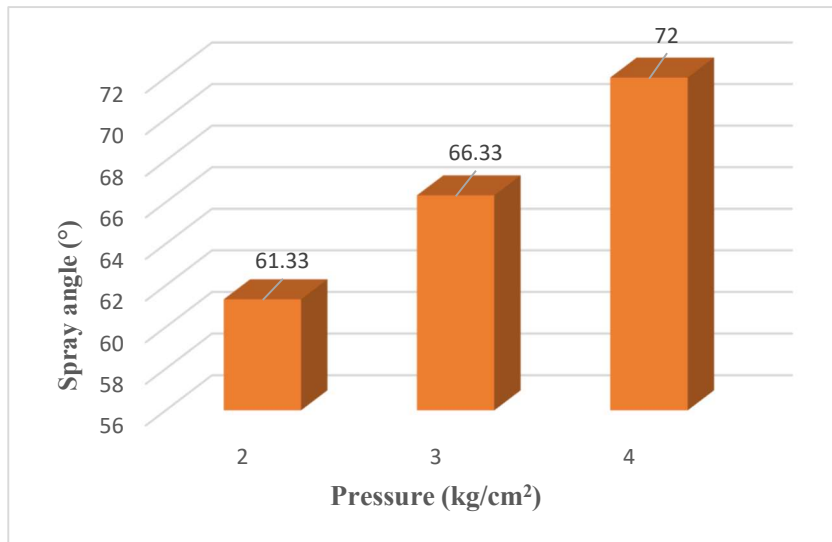


Fig 4.2: Effect of different pressures on angle of spray

4.1.1.3 Swath Width

The effect of different pressures and heights of nozzle on the swath width was observed and studied as shown in Table 4.1. It was observed that the swath width increased with increase in working pressure. Similarly, the swath width also increased with increase in nozzle height at each operating pressure.

Table 4.1: Effect of different pressures and nozzle heights on swath width

Nozzle height (cm)	Pressure (kg/cm ²)	Mean swath width (cm)
45	2.0	51.00
	3.0	57.00
	4.0	63.00
50	2.0	54.00
	3.0	60.00
	4.0	66.00
55	2.0	60.00
	3.0	63.00
	4.0	72.00

4.1.1.4 Spray distribution pattern

The hollow cone nozzle was tested at the patterator and it was observed that maximum amount of liquid collected at the central region while it decreased at the outer ends of the spray pattern. The volume of liquid collected at each channels are given in Appendix A1 to A3. The spray distribution at different pressures and nozzle heights is shown in Fig 4.3 to 4.5.

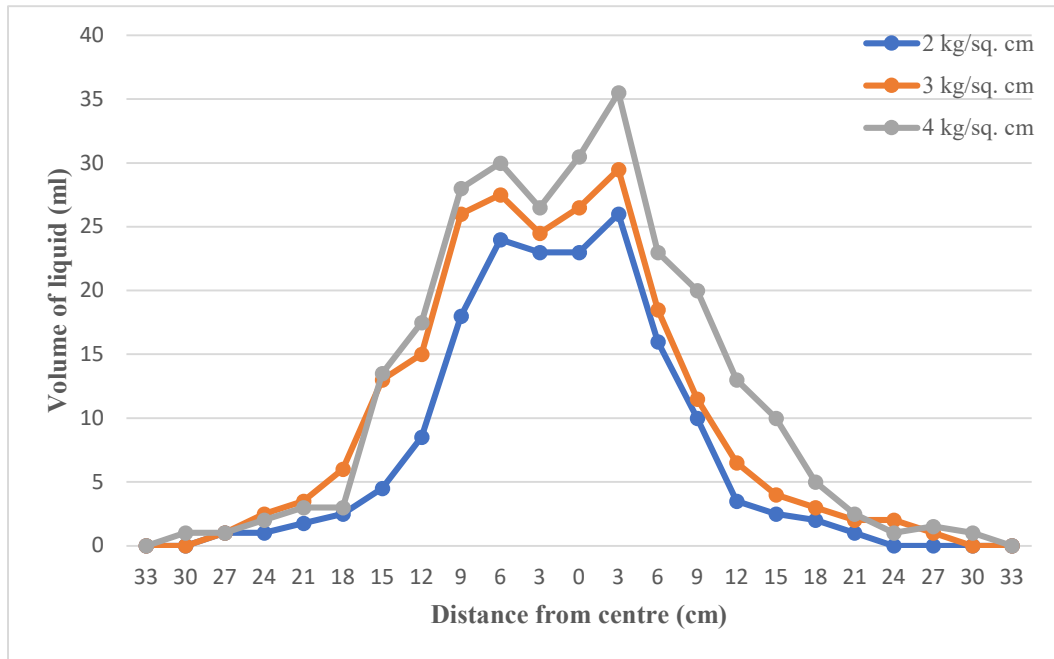


Fig 4.3: Spray distribution at 45 cm nozzle height

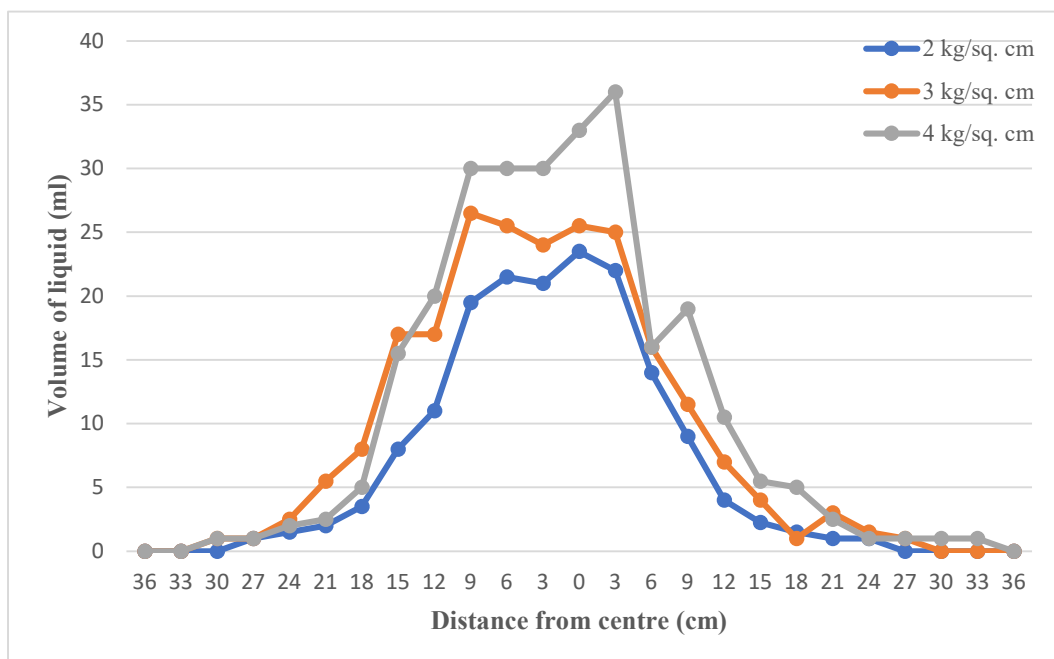


Fig 4.4: Spray distribution at 50 cm nozzle height

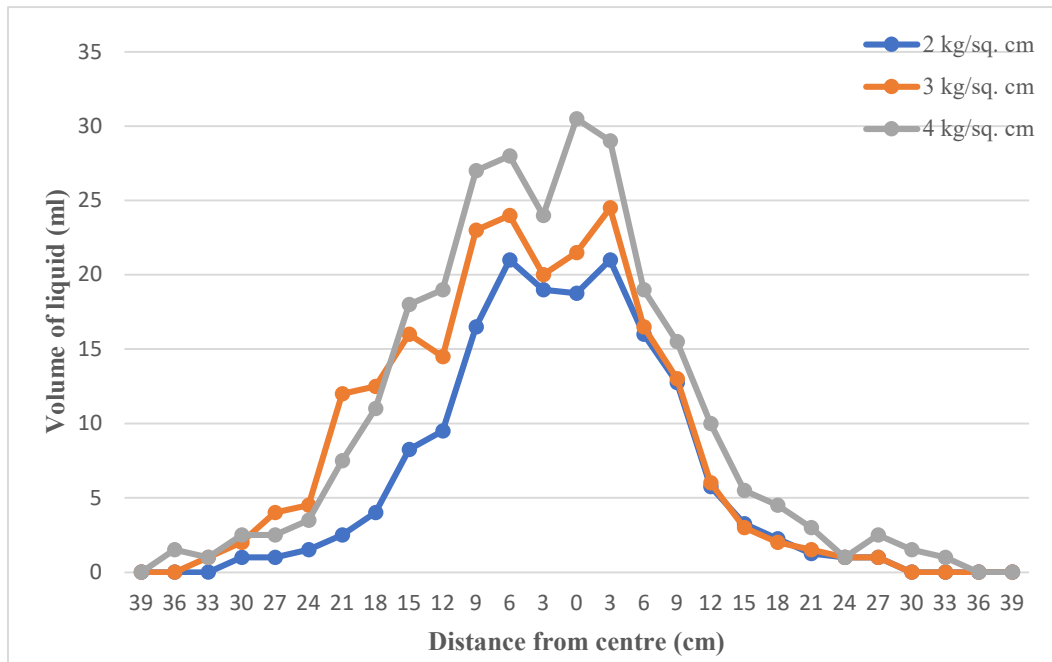


Fig 4.5: Spray distribution at 55 cm nozzle height

4.1.2 Nozzle spacing

By overlapping the spray distribution pattern, the coefficient of variation (CV) of spray distribution between centre to centre of two nozzles were theoretically calculated as shown in Table 4.2. After calculation it was observed that coefficient of variation was minimum at pressure of 3 kg/cm² when operated at a nozzle height of 55 cm. Hence, nozzle pressure of 3 kg/cm² and nozzle height of 55 cm was found to be the best combination for operating the solar PV assisted sprayer under field condition because it generated the lowest CV. Simultaneously, at this pressure & nozzle height combination, after overlapping and generation of minimum CV, nozzle spacing of 36 cm was selected for mounting of nozzles on spray boom.

Table 4.2: Minimum CV at different pressures and nozzle heights

Pressure (kg/cm ²)	Nozzle height (cm)	Minimum CV (%)	Nozzle Spacing (cm)
2.0	45	34.06	30
	50	35.17	30
	55	33.35	33
3.0	45	27.57	30
	50	28.37	33
	55	23.36	36
4.0	45	28.62	33
	50	35.14	33
	55	35.77	39

4.2 Performance evaluation of the solar PV setup

The performance evaluation was carried out on 30 January, 2021, using a 100 Wp solar panel. The relevant parameters were observed and recorded from 9:00 am to 05:00 pm using the required instruments while the array output and conversion efficiency were calculated as shown in Table 4.3.

Table 4.3: Recorded observations on 30 January 2021

Time (h)	Solar irradiance (W/m ²)	Ambient temperature (°C)	Solar panel output voltage (V)	Solar panel output current (A)	Array output (W)	Panel surface temperature (°C)	Conversion efficiency (%)
09:00	179.30	9.0	12.2	1.9	23.18	21.9	20.20
09:30	275.60	13.0	12.6	2.0	25.20	23.0	14.29
10:00	378.10	16.0	12.8	2.2	28.16	25.1	11.64
10:30	430.50	16.0	12.9	2.4	30.96	26.0	11.24
11:00	469.50	17.0	13.2	2.5	33.00	28.3	10.98
11:30	499.20	17.0	13.3	2.9	38.57	30.7	12.07
12:00	480.10	18.0	12.9	2.6	33.54	31.1	10.91
12:30	540.50	18.0	13.2	4.6	60.72	28.8	17.55
13:00	583.90	19.0	13.2	4.8	63.36	27.1	16.95
13:30	540.90	19.0	13.3	4.8	63.84	26.7	18.44
14:00	533.80	20.0	13.2	4.6	60.72	27.3	17.77
14:30	570.10	18.0	13.2	4.5	59.40	30.3	16.28
15:00	403.80	18.0	13.0	3.7	48.10	28.1	18.61
15:30	327.90	17.0	12.9	3.1	39.99	25.8	19.05
16:00	254.50	17.0	12.7	2.5	31.75	23.9	19.49
16:30	193.60	16.0	12.5	2.0	25.00	21.6	20.18
17:00	137.80	15.0	12.3	1.5	18.45	20.8	20.92

4.2.1 Variation of array output with solar irradiance

The variation of array output due to the influence of solar irradiance has been shown in Fig 4.6. It was observed that the array output is minimum at the morning and then increased as the solar irradiance increased and again decreased to a minimum in the evening as the solar irradiance decreased. It was observed that the array output increased greatly from 12:30 pm to 02:30 pm which was mostly due to the direct irradiance of solar radiation on the panel surface which led to excitation of electrons on the panel structure leading to higher generation of voltage and current. The maximum array output of 63.84 W was observed at 01:30 pm while the minimum array output of 18.45 W was observed at 05:00 pm.

4.2.2 Variation of ambient temperature and panel temperature with time

The variation of ambient temperature and panel temperature during the whole day i.e. from 9:00 am to 5:00 pm is shown in Table 4.3. It was observed that the panel temperature increased with the increase in ambient temperature and vice versa. The daytime temperature of a solar cell was not equal to the ambient temperature, since solar cells are dark in color and therefore absorb a greater portion of the sun's energy. Hence, during the day, a solar cell operated hotter than the ambient temperature which was in accordance with (Elminir *et al* 2001). However, during the noon time from 12:30 pm to 01:30 pm, the panel temperature showed a opposite trend even though the ambient temperature increased. This might be due to the action of wind blowing during that time which provided a cooling effect on the solar panel which decreased the temperature.

4.2.3 Variation of conversion efficiency

The variability of conversion efficiency is shown in Fig 4.7. It can be observed that conversion efficiency showed an inverse trend in relation to panel temperature. The maximum conversion efficiency of 20.92% was observed at 05:00 pm when the panel temperature was 20.8°C while minimum conversion efficiency of 10.91% was observed at 12:00 pm when the panel temperature was 31.1°C. Hence, it can be said that solar panel performed better at lower panel temperatures which was again due to the influence of lower ambient temperatures. Due to lower panel temperature, the voltage generation increased resulting in higher array output which led to increase in conversion efficiency and these results are in accordance with (Vashist *et al* 2016). However it was observed that the conversion efficiency improved from 12:30 pm to 02:30 pm. The major reason for this improvement had less to do with panel temperature and more to do with the output current. Except from 12:30 pm to 02:30 pm, at higher panel temperatures, the conversion efficiency of the solar panel decreased which was due to generation of heat in the panel due to absorption, leading to loss of useful electrical power as heat, which was also reported by (Dubey *et al* 2012). Higher solar irradiance increases the

output power, but this effect was partly counterbalanced by the effect of the PV panel temperature (above 25°C) which reduced the efficiency (Amelia *et al* 2016). Similar effects of panel temperature on conversion efficiency were also observed by (El-Adaw *et al* 2015, Kumar *et al* 2019 and Li *et al* 2021).

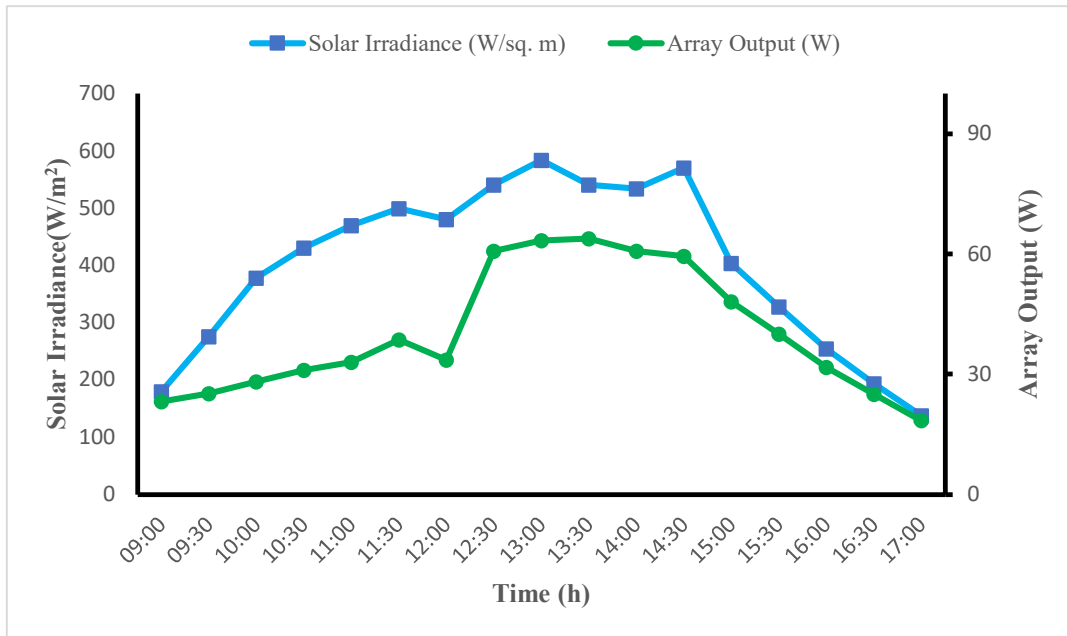


Fig 4.6: Variation of solar irradiance and array output with time

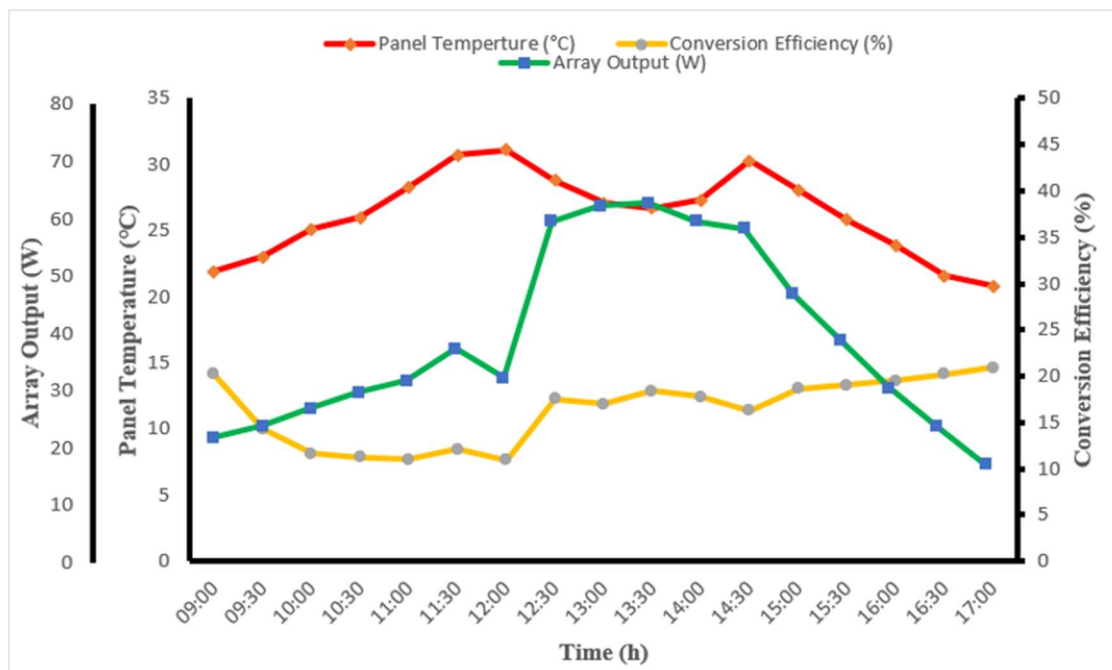


Fig 4.7: Variation of array output, panel temperature and conversion efficiency with time

4.3 Field evaluation of the SPV assisted sprayer mounted on a self propelled carrier

The developed SPV assisted sprayer mounted on a self propelled carrier was evaluated in wheat crop for field parameters and spray parameters.

4.3.1 Field parameters

4.3.1.1 Swath width

The swath width at field conditions were measured at two forward speeds and different number of nozzles. It was observed that there was no effect of forward speeds on the swath width. Hence, the swath width was measured considering only one forward speed (0.6 m/s) and taking different number of nozzles. The swath increased with the increase in number of nozzles. While working with 4, 6 and 8 number of nozzles, the overall swath width was 172.00 cm, 245.10 cm and 316.30 cm respectively.

4.3.1.2 Application rate

The application rate was calculated at different forward speeds considering only 8 number of nozzles in the boom. The discharge from each nozzle of the boom, starting from left to right, as shown in Table 4.4 was noted to calculate the average discharge from the boom also shown in Fig 4.8. The application rate decreased with the increase in forward speed. The application rate was found to be 156.23 l/ha at forward speed of 0.6 m/s and 133.91 l/ha at 0.7 m/s. The application rate at forward speed of 0.6 m/s was within the application rate recommended in package of practices for Rabi crops of Punjab (Anonymous 2020), required for Aphids in wheat crop.

Table 4.4: Total and average discharge from the nozzles of boom

Nozzle Nos.	Mean Discharge (ml/min)
1	219.00
2	217.67
3	220.00
4	228.67
5	226.67
6	226.33
7	223.33
8	217.33
Average discharge rate (ml/min)	222.38
Total discharge rate (l/min)	1.779

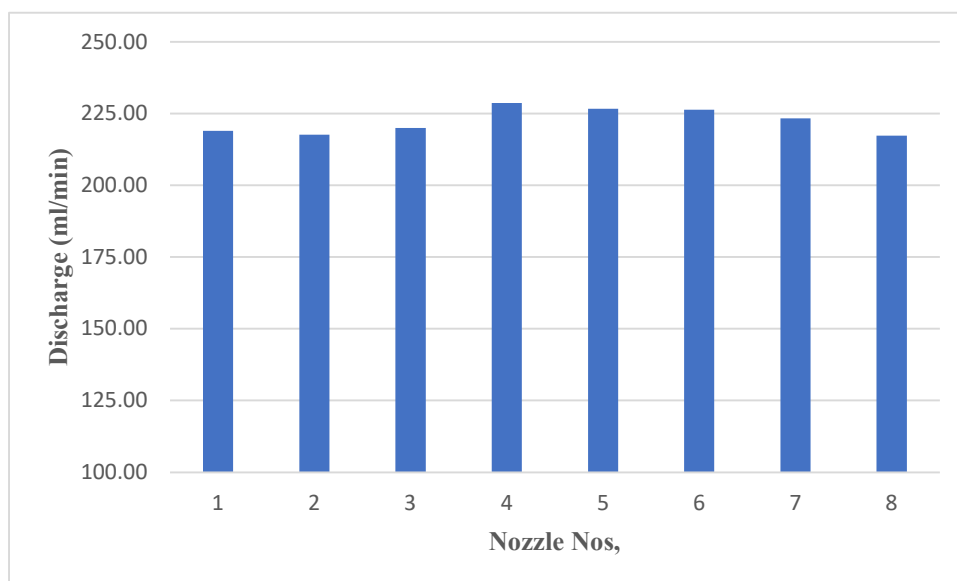


Fig 4.8: Discharge variation from every nozzles of boom

4.3.1.3 Field capacity

The theoretical and actual field capacity of the developed sprayer at various forward speeds and number of nozzles is shown in Table 4.5. It can be observed that both theoretical field capacity and actual field capacity increased with increase forward speed and number of nozzles. The maximum field capacities were observed at a combination of 0.7 m/s forward speed and 8 number of nozzles.

Table 4.5: Field capacities at different forward speeds and number of nozzles

Forward speed(m/s)	Number of nozzles	Theoretical field capacity (ha/h)	Actual field capacity (ha/h)
0.6	4	0.36	0.28
	6	0.51	0.39
	8	0.65	0.49
0.7	4	0.42	0.33
	6	0.59	0.46
	8	0.77	0.59

4.3.1.4 Field Efficiency

Field efficiency of the developed SPV sprayer was found to be in the range of 74.81–79.90 %.

4.3.2 Spray parameters

4.3.2.1 Droplet size and uniformity coefficient

4.3.2.1.1 Number median diameter (NMD)

4.3.2.1.1.1 NMD at top canopy of wheat

The effect of different nozzle pressures and forward speeds on NMD at top canopy of wheat crop were observed and tabulated in Table 4.6. The NMD at different nozzle pressures and forward speeds on upper side of leaves varied from 93.25 μm to 157.12 μm at top canopy of wheat crop while on the underside of the leaves it varied from 70.33 μm to 131.22 μm . The NMD tends to decrease with the increase in pressure which was similar to the trend observed by (Jassowal *et al* 2016).

ANOVA for effect of pressure and forward speed on NMD at top canopy is shown in Appendix B1 and B2. The statistical analysis showed that pressure had a significant effect on the NMD at top canopy of the wheat crop (upper side and under side) while the forward speed had no significant effect on the NMD at top canopy (upper side and under side) (Table 4.7). Also, interaction of pressure and forward speed had no significant effect on the NMD at both upper side and under side of top canopy of wheat.

Table 4.6: NMD (μm) at top canopy of wheat

Pressure (kg/cm²)	Forward Speed (m/s)	Upper side of leaves NMD (μm)	Under side of leaves NMD (μm)
2	0.6	149.23	119.38
	0.7	157.12	131.22
3	0.6	117.97	100.87
	0.7	124.79	90.42
4	0.6	102.61	80.35
	0.7	93.25	70.33

Table 4.7: Significance of pressure and forward speed on NMD at top canopy

Source	Upper side		Underside	
	F Value	Pr > F	F Value	Pr > F
Pressure	7.10	0.0093 ^S	17.03	0.0003 ^S
Forward Speed	0.02	0.8845 ^{NS}	0.17	0.6895 ^{NS}
Pressure*Forward Speed	0.22	0.8092 ^{NS}	1.10	0.3655 ^{NS}
NS = Non Significant, S = Significant				

4.3.2.1.1.2 NMD at middle canopy of wheat

Effect of different nozzle pressures and forward speeds on NMD at middle canopy of wheat crop were observed and tabulated in Table 4.8. The NMD at different nozzle pressures and forward speeds on upper side of leaves varied from 98.39 μm to 159.13 μm at middle canopy of wheat crop while on the underside of the leaves it varied from 69.89 μm to 121.67 μm . NMD decreased with the increase in pressure.

ANOVA for effect of pressure and forward speed on NMD at middle canopy is shown in Appendix B3 and B4. The statistical analysis showed that pressure had a significant effect on the NMD at middle canopy of the wheat crop (upper side and under side) while the forward speed had no significant effect on the NMD at middle canopy (upper side and under side) (Table 4.9). Also, interaction of pressure and forward speed had no significant effect on the NMD at both upper side and under side of middle canopy of wheat.

Table 4.8: NMD (μm) at middle canopy of wheat

Pressure (kg/cm^2)	Forward Speed (m/s)	Upper side of leaves NMD (μm)	Under side of leaves NMD (μm)
2	0.6	159.13	115.62
	0.7	145.22	121.67
3	0.6	131.41	97.32
	0.7	115.93	90.31
4	0.6	105.63	79.62
	0.7	98.39	69.89

Table 4.9: Significance of pressure and forward speed on NMD at middle canopy

Source	Upper side		Underside	
	F Value	Pr > F	F Value	Pr > F
Pressure	13.43	0.0009 ^S	67.97	<.0001 ^S
Forward Speed	2.37	0.1495 ^{NS}	1.34	0.2703 ^{NS}
Pressure*Forward Speed	0.10	0.9042 ^{NS}	2.50	0.1239 ^{NS}

NS = Non Significant, S = Significant

4.3.2.1.2 Volume median diameter (VMD)**4.3.2.1.2.1 VMD at top canopy of wheat**

The effect of different nozzle pressures and forward speeds on VMD at top canopy of wheat crop were observed and tabulated in Table 4.10. The VMD at different nozzle pressures and forward speeds on upper side of leaves varied from 196.33 μm to 255.33 μm at top canopy of wheat crop while on the underside of the leaves it varied from 159.33 μm to 233.33 μm . It was observed that VMD tends to decrease with the increase in pressure. Similar trend was observed by (Jassowal *et al* 2016).

ANOVA for effect of pressure and forward speed on VMD at top canopy is shown in Appendix B5 and B6. The statistical analysis showed that pressure had a significant effect on the VMD at top canopy of the wheat crop (upper side and under side) while the forward speed had no significant effect on the VMD at top canopy (upper side and under side) (Table 4.11). Also, interaction of pressure and forward speed had no significant effect on the VMD at both upper side and under side of top canopy of wheat.

Table 4.10: VMD (μm) at top canopy of wheat

Pressure (kg/cm^2)	Forward Speed (m/s)	Upper side of leaves VMD (μm)	Under side of leaves VMD (μm)
2	0.6	255.33	233.33
	0.7	246.33	222.67
3	0.6	208.33	182.33
	0.7	230.67	191.33
4	0.6	210.67	170.33
	0.7	196.33	159.33

Table 4.11: Significance of pressure and forward speed on VMD at top canopy

Source	Upper side		Underside	
	F Value	Pr > F	F Value	Pr > F
Pressure	6.43	0.0127 ^S	19.71	0.0002 ^S
Forward Speed	0.00	0.9762 ^{NS}	0.26	0.6218 ^{NS}
Pressure*Forward Speed	1.09	0.3679 ^{NS}	0.63	0.5501 ^{NS}

NS = Non Significant, S = Significant

4.3.2.1.2.2 VMD at middle canopy of wheat

Effect of different nozzle pressures and forward speeds on VMD at middle canopy of wheat crop were observed and tabulated in Table 4.12. The VMD at different nozzle pressures and forward speeds on upper side of leaves varied from 185.33 μm to 251.67 μm at middle canopy of wheat crop while on the underside of the leaves it varied from 153.67 μm to 228.67 μm . The VMD was observed to be decreasing with the increase in pressure.

ANOVA for effect of pressure and forward speed on VMD at middle canopy is shown in Appendix B7 and B8. The statistical analysis showed that pressure had a significant effect on the VMD at middle canopy of the wheat crop (upper side and under side) while the forward speed had no significant effect on the VMD at middle canopy (upper side and under side) (Table 4.13). Also, interaction of pressure and forward speed had no significant effect on the VMD at both upper side and under side of middle canopy of wheat.

Table 4.12: VMD (μm) at middle canopy of wheat

Pressure (kg/cm ²)	Forward Speed (m/s)	Upper side of leaves VMD (μm)	Under side of leaves VMD (μm)
2	0.6	251.67	228.67
	0.7	244.33	217.67
3	0.6	210.33	185.33
	0.7	220.67	191.67
4	0.6	198.67	167.33
	0.7	185.33	153.67

Table 4.13: Significance of pressure and forward speed on VMD at middle canopy

Source	Upper side		Underside	
	F Value	Pr > F	F Value	Pr > F
Pressure	12.79	0.0011 ^S	22.54	<.0001 ^S
Forward Speed	0.14	0.7110 ^{NS}	0.64	0.4390 ^{NS}
Pressure*Forward Speed	0.61	0.5582 ^{NS}	0.67	0.5278 ^{NS}

NS = Non Significant, S = Significant

4.3.2.1.3 Uniformity coefficient (UC)**4.3.2.1.3.1 UC at top canopy of wheat**

The UC was calculated for different pressures and forward speeds at top canopy of wheat crop as shown in Table 4.14. The UC varied from 1.59 to 2.13 at upper side and 1.70 to 2.32 at under side of leaves at top canopy of wheat crop.

ANOVA for effect of pressure and forward speed on UC at top canopy is shown in Appendix B9 and B10. The statistical analysis showed that pressure and forward speed had no significant effect on the UC at top canopy (upper side and under side) (Table 4.15). Also, interaction of pressure and forward speed had no significant effect on the UC at both upper side and under side of top canopy of wheat.

Table 4.14: UC at top canopy of wheat

Pressure (kg/cm ²)	Forward Speed (m/s)	Upper side of leaves UC	Under side of leaves UC
2	0.6	1.71	1.96
	0.7	1.59	1.70
3	0.6	1.80	1.83
	0.7	1.99	2.16
4	0.6	2.13	2.19
	0.7	2.11	2.32

Table 4.15: Significance of pressure and forward speed on UC at top canopy

Source	Upper side		Underside	
	F Value	Pr > F	F Value	Pr > F
Pressure	2.41	0.1316 ^{NS}	2.47	0.1261 ^{NS}
Forward Speed	0.01	0.9246 ^{NS}	0.19	0.6746 ^{NS}
Pressure*Forward Speed	0.29	0.7506 ^{NS}	1.23	0.3279 ^{NS}

NS = Non Significant

4.3.2.1.3.2 UC at middle canopy of wheat

The UC was also calculated for different pressures and forward speeds at middle canopy of wheat crop as shown in Table 4.16. The UC varied from 1.60 to 1.93 at upper side and 1.80 to 2.20 at under side of leaves at middle canopy of wheat crop.

ANOVA for effect of pressure and forward speed on UC at middle canopy is shown in Appendix B11 and B12. The statistical analysis showed that pressure and forward speed had no significant effect on the UC at middle canopy (upper side and under side) (Table 4.17). Also, interaction of pressure and forward speed had no significant effect on the UC at both upper side and under side of middle canopy of wheat.

Table 4.16: UC at middle canopy of wheat

Pressure (kg/cm ²)	Forward Speed (m/s)	Upper side of leaves UC	Under side of leaves UC
2	0.6	1.60	1.98
	0.7	1.74	1.80
3	0.6	1.61	1.91
	0.7	1.93	2.13
4	0.6	1.88	2.11
	0.7	1.90	2.20

Table 4.17: Significance of pressure and forward speed on UC at middle canopy

Source	Upper side		Underside	
	F Value	Pr > F	F Value	Pr > F
Pressure	0.85	0.4506 ^{NS}	2.19	0.1546 ^{NS}
Forward Speed	1.40	0.2590 ^{NS}	0.17	0.6885 ^{NS}
Pressure*Forward Speed	0.42	0.6666 ^{NS}	1.38	0.2900 ^{NS}

NS = Non Significant

4.3.2.2 Spray deposition

The spray deposition can be defined in terms of droplet density (droplets/cm²), spray coverage area (%) and ground losses (µl/cm²).

4.3.2.2.1 Droplet density

4.3.2.2.1.1 Droplet density at top canopy of wheat

The droplet density at different nozzle pressures and forward speeds on upper side of leaves in the top canopy of wheat crop varied from 51.03 to 117.67 droplets/cm² (Table 4.18). Droplet density at the underside of the leaves at top canopy varied from 8.67 to 29.87 droplets/cm², which was quite less compared to the droplet density at the upper side of leaves. The droplet density increased with the increase in pressure as it led production of more number of finer droplets whereas the droplet density decreased with the increase in forward speed which might be due to lesser duration of exposure. The maximum droplet density at upper side and underside of top canopy, 117.67 droplets/cm² and 29.87 droplets/cm², was observed at pressure of 4 kg/cm² and 0.6 m/s forward speed. The minimum droplet density on both upper side and under side of top canopy of wheat was observed at pressure of 2 kg/cm² and 0.7 m/s forward speed.

ANOVA for effect of pressure and forward speed on droplet density at top canopy is shown in Appendix B13 and B14. The statistical analysis showed that both pressure and forward speed had significant effect on the droplet density at top canopy (upper side and under side) (Table 4.19). But, interaction of pressure and forward speed didn't had significant effect on the droplet density at both upper side and under side of top canopy of wheat.

Table 4.18: Droplet density at top canopy of wheat

Pressure (kg/cm²)	Forward Speed (m/s)	Upper side of leaves (droplets/cm²)	Under side of leaves (droplets/cm²)
2	0.6	60.73	13.00
	0.7	51.03	8.67
3	0.6	82.83	21.47
	0.7	66.63	15.83
4	0.6	117.67	29.87
	0.7	95.37	23.67

Table 4.19: Significance of pressure and forward speed on droplet density at top canopy

Source	Upper side		Underside	
	F Value	Pr > F	F Value	Pr > F
Pressure	38.95	<.0001 ^S	40.04	<.0001 ^S
Forward Speed	11.52	0.0053 ^S	13.74	0.0030 ^S
Pressure*Forward Speed	0.59	0.5694 ^{NS}	0.14	0.8670 ^{NS}

NS = Non Significant, S = Significant

4.3.2.2.1.2 Droplet density at middle canopy of wheat

The effect of nozzle pressure and forward speed on droplets density on middle canopy of wheat crop has been shown in Table 4.20. The droplet density on upper side of leaves in the middle canopy of wheat crop varied from 43.33 to 100.27 droplets/cm². Droplet density at the underside of the leaves at middle canopy varied from 3.97 to 22.63 droplets/cm², which was quite less compared to the droplet density at the upper side of leaves. The droplet density increased with the increase in pressure as it led production of more number of finer droplets whereas the droplet density decreased with the increase in forward speed which might be due to lesser duration of exposure. The maximum droplet density at upper side and underside of middle canopy, 100.27 droplets/cm² and 22.63 droplets/cm², was observed at pressure of 4 kg/cm² and 0.6 m/s forward speed. The minimum droplet density on both upper side and under side of middle canopy of wheat was observed at pressure of 2 kg/cm² and 0.7 m/s forward speed.

ANOVA for effect of pressure and forward speed on droplet density at middle canopy is shown in Appendix B15 and B16. The statistical analysis showed that both pressure and forward speed had significant effect on the droplet density at middle canopy (upper side and under side) (Table 4.21). But, interaction of pressure and forward speed didn't had significant effect on the droplet density at both upper side and under side of middle canopy of wheat.

Table 4.20: Droplet density at middle canopy of wheat

Pressure (kg/cm ²)	Forward Speed (m/s)	Upper side of leaves (droplets/cm ²)	Under side of leaves (droplets/cm ²)
2	0.6	51.63	7.67
	0.7	43.33	3.97
3	0.6	76.87	15.67
	0.7	63.67	10.13
4	0.6	100.27	22.63
	0.7	85.13	16.87

Table 4.21: Significance of pressure and forward speed on droplet density at middle canopy

Source	Upper side		Underside	
	F Value	Pr > F	F Value	Pr > F
Pressure	80.63	<.0001 ^S	54.74	<.0001 ^S
Forward Speed	17.64	0.0012 ^S	21.15	0.0006 ^S
Pressure*Forward Speed	0.49	0.6248 ^{NS}	0.36	0.7042 ^{NS}

NS = Non Significant, S = Significant

4.3.2.2.2 Spray coverage area (%)

4.3.2.2.2.1 Spray coverage area (%) at top canopy of wheat

The effect of nozzle pressure and forward speed on spray coverage area (%) on top canopy of wheat crop has been shown in Table 4.22. The % area coverage on upper side of leaves in the top canopy of wheat crop varied from 10.19 to 15.90 %. Area coverage (%) at the underside of the leaves at top canopy varied from 0.76 to 4.01 %. The spray coverage area increased with the increase in pressure which might be due to the production of more number of finer droplets which spread over a larger area. The maximum % area coverage at upper side and underside of top canopy, 15.90 % and 4.01 %, was observed at pressure of 4 kg/cm² and 0.6 m/s forward speed. The minimum % area coverage on both upper side and under side of top canopy of wheat was observed at pressure of 2 kg/cm² and 0.7 m/s forward speed.

ANOVA for effect of pressure and forward speed on spray coverage area at top canopy is shown in Appendix B17 and B18. The statistical analysis showed that pressure had a significant effect on the % area coverage on both upper side and under side of the top canopy whereas the effect of forward speed on % area coverage was not significant at top canopy (upper side and under side) (Table 4.23). Also, interaction of pressure and forward speed had no significant effect on the % spray area coverage at both upper side and under side of top canopy of wheat.

Table 4.22: Coverage area (%) at top canopy of wheat

Pressure (kg/cm ²)	Forward Speed (m/s)	Upper side of leaves	Under side of leaves
2	0.6	11.23	1.10
	0.7	10.19	0.76
3	0.6	14.02	2.76
	0.7	12.80	2.30
4	0.6	15.90	4.01
	0.7	14.61	3.19

Table 4.23: Significance of pressure and forward speed on coverage area at top canopy

Source	Upper side		Underside	
	F Value	Pr > F	F Value	Pr > F
Pressure	5.43	0.0209 ^S	19.32	0.0002 ^S
Forward Speed	1.09	0.3166 ^{NS}	2.35	0.1510 ^{NS}
Pressure*Forward Speed	0.00	0.9957 ^{NS}	0.17	0.8495 ^{NS}

NS = Non Significant, S = Significant

4.3.2.2.2.1 Spray coverage area(%) at middle canopy of wheat

The effect of nozzle pressure and forward speed on spray coverage area (%) on middle canopy of wheat crop has been shown in Table 4.24. The % area coverage on upper side of leaves in the middle canopy of wheat crop varied from 9.23 to 14.87 %. Area coverage (%) at the underside of the leaves at middle canopy varied from 0.59 to 3.25 %. The spray coverage area increased with the increase in pressure which might be due to the production of more number of finer droplets which spread over a larger area. The maximum % area coverage at upper side and underside of middle canopy, 14.87 % and 3.25 %, was observed at pressure of 4 kg/cm² and 0.6 m/s forward speed. The minimum % area coverage on both upper side and under side of middle canopy of wheat was observed at pressure of 2 kg/cm² and 0.7 m/s forward speed.

ANOVA for effect of pressure and forward speed on spray coverage area at middle canopy is shown in Appendix B19 and B20. The statistical analysis showed that pressure had a significant effect on the % area coverage on both upper side and under side of the middle canopy whereas the effect of forward speed on % area coverage was not significant at middle canopy (upper side and under side) (Table 4.25). Also, interaction of pressure and forward speed had

no significant effect on the % spray area coverage at both upper side and under side of middle canopy of wheat.

Table 4.24: Coverage area (%) at middle canopy of wheat

Pressure (kg/cm ²)	Forward Speed (m/s)	Upper side of leaves	Under side of leaves
2	0.6	10.11	0.93
	0.7	9.23	0.59
3	0.6	12.98	2.00
	0.7	11.36	1.51
4	0.6	14.87	3.25
	0.7	12.93	2.42

Table 4.25: Significance of pressure and forward speed on coverage area at middle canopy

Source	Upper side		Underside	
	F Value	Pr > F	F Value	Pr > F
Pressure	7.12	0.0092 ^S	10.70	0.0021 ^S
Forward Speed	2.58	0.1339 ^{NS}	2.28	0.1568 ^{NS}
Pressure*Forward Speed	0.12	0.8916 ^{NS}	0.16	0.8568 ^{NS}

NS = Non Significant, S = Significant

4.3.2.2.3 Ground losses

The effect of nozzle pressure and forward speed on ground losses ($\mu\text{l}/\text{cm}^2$) is shown Table 4.26. It was observed that the ground losses decreased with the increase in nozzle pressure. It might be due higher dispersion of finer droplets at higher pressure causing the droplets to adhere well to the canopy of the crop rather than dropping down to the ground. The maximum ground loss was found to be $0.765 \mu\text{l}/\text{cm}^2$ at nozzle pressure of $2 \text{ kg}/\text{cm}^2$ and forward speed of $0.6 \text{ m}/\text{s}$ while the minimum ground loss was $0.446 \mu\text{l}/\text{cm}^2$ at nozzle pressure of $4 \text{ kg}/\text{cm}^2$ and forward speed of $0.7 \text{ m}/\text{s}$.

ANOVA for effect of pressure and forward speed on ground losses is shown in Appendix B21. The statistical analysis showed that pressure had a significant effect on the ground losses whereas the effect of forward speed on ground losses was not significant (Table

4.27). Also, interaction of pressure and forward speed had no significant effect on the ground losses.

Table 4.26: Ground losses

Pressure (kg/cm²)	Forward speed (m/s)	Ground losses (µl/cm²)
2	0.6	0.765
	0.7	0.729
3	0.6	0.599
	0.7	0.565
4	0.6	0.466
	0.7	0.446

Table 4.27: Significance of pressure and forward speed on ground losses

Source	F Value	Pr > F
Pressure	9.87	0.0029 ^S
Forward speed	0.31	0.5863 ^{NS}
Pressure*Forward speed	0.01	0.9912 ^{NS}
NS = Non Significant, S = Significant		

CHAPTER V

SUMMARY

Solar energy is a clean, renewable, everlasting energy source having no potential damage on the environment. India is gifted with a vast potential in solar energy. Solar energy of around 4 to 7 kWh/m² per day is available on India's soil. In Punjab region, the average annual solar radiation is about 5.32 kWh/m²/day. As solar radiation is abundantly available, the electricity produced from solar photovoltaic (SPV) system can be used to power various farm devices/operations.

One of the important operation in agricultural field is plant protection. Optimum utilization of pesticides in field can be achieved using sprayers with minimum efforts. Indian farms generally use two types of spraying pumps, which are fuel operated and hand operated type, among which hand operated spraying pumps are most prevalent. Hand operated sprayer leads to higher human efforts whereas fuel operated leads to higher cost of operation and pollution. Hence, the technology of solar energy can be extended for spraying pesticides, fungicides, fertilizers, nutrients and weedicides using solar sprayers.

As of now the solar operated sprayers which have been developed has basically been backpack type or manual push type. However, these types of sprayers increases the drudgery on the operator for longer duration of operation. A completely solar operated self propelled sprayer is not economically viable due to its high initial investment. Also, it is very difficult to mount more number of solar panels in a moving agricultural vehicle due to uneven terrains in fields making it most likely to damages.

Hence, an initiative was undertaken to develop and evaluate a solar photo voltaic assisted sprayer which was mounted on a self propelled carrier driven by a diesel engine. Wheat was selected as the target crop for evaluation of the developed sprayer. Wheat (*Triticum aestivum* L.) is one of the major staple crop grown in India with Punjab being the second largest producer within the country with a production of about 17.35 MT. A suitable electrically operated diaphragm type pump motor combo available in the local market was selected for spraying operation. Depending on the power requirement to operate the pump motor and solar power availability in Ludhiana, Punjab, during the winters, theoretical calculation was done for battery and solar panel requirements. Pulse Width Modulation (PWM) type solar charge controller capable of withstanding 12/24 V load and 40 A current was selected for controlling the voltage coming from the solar panel to the battery. Simultaneously, depending on the pressure and discharge of the pump motor combo, hollow cone nozzles (TXA800050VK) of TeeJet Technologies were selected for development of boom of the sprayer.

To select suitable operational parameters, the selected nozzle was tested in laboratory in a patternator at three different pressures (2, 3 and 4 kg/cm²) and three different nozzle heights

(45, 50 and 55 cm). Discharge, spray angle, swath width and spray distribution pattern were studied during the laboratory study. The spray distribution pattern helped in determining the minimum coefficient of variation at all pressure height combinations by overlapping one pattern over other. The minimum coefficient of variation was calculated for determining the spacing of the nozzles in the boom.

The best combination of pressure and nozzle height as selected from laboratory evaluation was selected for evaluation of the solar photo voltaic setup and determination of field parameters like swath width, application rate, field capacity and field efficiency. From initial testing of the spray boom for a typical day (8 hours) of operation, it was observed that a 12 V 26 Ah lead acid battery was sufficient for operating the spraying system and simultaneously solar panel of 100 Wp was selected for charging the battery. The evaluation of solar photo voltaic setup was conducted on 31 January, 2021 to determine the array output and the conversion efficiency of the solar panel. The evaluation of field parameters was performed taking two different forward speeds (0.6 and 0.7 m/s) and three different number of nozzles (4, 6 and 8).

The spray parameters were then evaluated at three different pressures (2, 3 and 4 kg/cm²) at nozzle heights based on minimum coefficient of variation and two different forward speeds (0.6 and 0.7 m/s). Water sensitive papers were mounted on stands in wheat field at top canopy, middle canopy and some close to the ground and then spraying operation was conducted. The papers were then collected for scanning and analyzed using DepositScan software. Spray parameters like VMD, NMD, uniformity coefficient, droplet density, % spray coverage area and ground losses were then determined.

Based on the results obtained from laboratory and field experiments following conclusions were drawn :

1. Based on spray distribution pattern, the minimum coefficient of variation was calculated at every pressure and height combination. It was observed that the minimum coefficient of variation of 23.36% was observed at pressure of 3 kg/cm² at nozzle height of 55 cm.
2. At other pressures i.e. at 2 kg/cm², the minimum coefficient of variation of 33.35% was observed at 55 cm nozzle height whereas at 4 kg/cm², the minimum coefficient of variation of 28.62% was observed at 45 cm nozzle height.
3. The solar photo voltaic setup was evaluated at 30th January, 2021 from 9:00 am to 5:00 pm and maximum solar irradiance of 559.30 W/m² was attained at 1:00 pm.
4. The panel temperature increased with the increase in ambient temperature and vice versa. Maximum panel temperature of 31.1°C was observed at 12:00 pm. During the noon time from 12:30 pm to 01:30 pm, the panel temperature showed a opposite trend

with respect to ambient temperature, which might be due to the effect of blowing wind which caused cooling effect.

5. The maximum array output of 63.84 W was observed at 01:30 pm while the minimum array output of 18.45 W was observed at 05:00 pm.
6. The conversion efficiency and panel temperature shared an inverse relationship. The maximum conversion efficiency of 20.92 % was observed at 05:00 pm when the panel temperature was 20.8°C while minimum conversion efficiency of 10.91% was observed at 12:00 pm when the panel temperature was 31.1°C.
7. Maximum swath width of 316.30 cm was observed while operating using 8 nozzles.
8. The application rate decreased from 156.23 to 133.91 l/ha when the forward capacity was increased from 0.6 to 0.7 m/s.
9. The maximum actual field capacity of 0.59 ha/h was observed at a combination of 0.7 m/s forward speed and 8 number of nozzles.
10. Field efficiency of the developed SPV sprayer mounted on a self propelled carrier was found to be in the range of 74.81–79.90 %.
11. The NMD at different nozzle pressures and forward speeds on top canopy of wheat crop at upper side of leaves varied from 93.25 μm to 157.12 μm while on the underside of the leaves it varied from 70.33 μm to 131.22 μm . The NMD at different nozzle pressures and forward speeds on middle canopy of wheat at upper side of leaves varied from 98.39 μm to 159.13 μm while on the underside of the leaves it varied from 69.89 μm to 121.67 μm .
12. The VMD at different nozzle pressures and forward speeds on upper side of leaves varied from 196.33 μm to 255.33 μm at top canopy of wheat crop while on the underside of the leaves it varied from 159.33 μm to 233.33 μm . The VMD at different nozzle pressures and forward speeds on upper side of leaves varied from 185.33 μm to 251.67 μm at middle canopy of wheat while on the underside of the leaves it varied from 153.67 μm to 228.67 μm .
13. The UC varied from 1.59 to 2.13 at upper side and 1.70 to 2.32 at under side of leaves at top canopy of wheat crop. Whereas, the UC varied from 1.60 to 1.93 at upper side and 1.80 to 2.20 at under side of leaves at middle canopy of wheat crop.
14. The droplet density at different nozzle pressures and forward speeds on upper side of leaves in the top canopy of wheat crop varied from 51.03 to 117.67 droplets/cm², whereas droplet density at the underside of the leaves varied from 8.67 to 29.87 droplets/cm², which was quite less compared to the droplet density at the upper side of leaves. The droplet density on upper side of leaves in the middle canopy of wheat crop varied from 43.33 to 100.27 droplets/cm², whereas droplet density at the underside of the leaves varied from 3.97 to 22.63 droplets/cm².

15. The % area coverage on upper side of leaves in the top canopy of wheat varied from 10.19 to 15.90 %, whereas area coverage (%) at the underside of the leaves varied from 0.76 to 4.01 %. The % area coverage on upper side of leaves in the middle canopy of wheat varied from 9.23 to 14.87 %, whereas area coverage (%) at the underside of the leaves varied from 0.59 to 3.25 %.
16. Ground losses decreased with the increase in nozzle pressure. The maximum ground loss was found to be $0.765 \mu\text{l}/\text{cm}^2$ at nozzle pressure of $2 \text{ kg}/\text{cm}^2$ and forward speed of 0.6 m/s while the minimum ground loss was $0.446 \mu\text{l}/\text{cm}^2$ at nozzle pressure of $4 \text{ kg}/\text{cm}^2$ and forward speed of 0.7 m/s .

SUGGESTIONS FOR FUTURE WORK

1. The engine of the developed machine can be replaced by a suitable electric motor to make the machine completely electric type.
2. Future studies can be undertaken for utilization of power from the solar panels during off season so that annual use of panels can be increased.
3. Economics and bio-efficacy of the developed sprayer needs to be studied.
4. Air assisted system can be incorporated in the spraying system for better deposition of spray droplets.

REFERENCES

- Aju, Adonis E S, Agbomabinu A E, Olah O S and Ibrahim S (2016) Development and performance evaluation of a trailed solar photovoltaic stand-alone system for rice threshing machine. *Int J Eng Res Technol* **5**:494-500.
- Amelia A R, Irwan Y M, Leow W Z, Irwanto M, Safwati I and Zhafarina M (2016) Investigation of the effect temperature on photovoltaic (PV) panel output performance. *Int J Adv Sci Eng Inf Technol* **6**:682-88.
- Anibude E C, Jahun R F and Abubakar M S (2016) Development of an animal drawn hydraulic boom sprayer. *A J Engg Res* **5**: 222-28.
- Anonymous (2004) *Self propelled light weight boom sprayer : A success story*. Pp 1-4. Central Institute of Agricultural Engineering, Bhopal.
- Anonymous (2019a) *India's oil import dependence jumps to 84 per cent*. <https://economictimes.indiatimes.com/industry/energy/oil-gas/indias-oil-import-dependence-jumps-to-84-pc/articleshow/69183923.cms>, accessed on 23 July, 2019.
- Anonymous (2019b) *Agricultural Statistics at a Glance 2018*. Government of India, Ministry of Agriculture & Farmers Welfare, Department of Agriculture, Cooperation & Farmers Welfare, Directorate of Economics and Statistics.
- Anonymous (2019c) *Solar resource maps of India*. <https://solargis.com/maps-and-gis-data/download/india>, accessed on 20 July, 2020.
- Anonymous (2020) *Package of practices for crops of Punjab (Rabi)*. Pp 14-15. Punjab Agricultural University, Ludhiana.
- Awulu J O and Sohoshan P Y (2012) Evaluation of a developed electrically operated knapsack sprayer. *Int J Sci Technol* **2**:769-72.
- Chandra Y P, Singh A, Kannojiya V and Kesari J P (2019) Solar energy a path to India's prosperity. *J Inst Eng India Ser C* **100**:539-46.
- Chandrashekar, Neeraja J and Raghavendra V (2018) Performance evaluation of solar operated push type sprayer. *Int J Curr Microbiol App Sci* **7**:1448-56.
- Chilundo R J, Mahanjane U S and Neves D (2018) Design and performance of photovoltaic water pumping systems: comprehensive review towards a renewable strategy for Mozambique. *J Power Energy Eng* **6**:32-63.

- Dawn S, Tiwari P K, Goswami A K and Mishra M K (2016) Recent developments of solar energy in India : Perspectives, strategies and future goals. *Renew Sustain Energy Rev* **62**: 215-35.
- Dubey S, Sarvaiya J N and Seshadri B (2013) Temperature dependent photovoltaic (PV) efficiency and its effect on PV production in the world - A review. *Energy Procedia* **33**:311-21.
- Ejaz K, Tahir A R, Khan F and Tariq M (2004) Performance evaluation of modified self levelling boom sprayer. *Int J Agric Bio* **6**: 636-38.
- El-Adaw M K, Shalaby S A, El-Ghany S E S A and Attallah M A (2015) Effect of solar cell temperature on its photovoltaic conversion efficiency. *Int J Sci Eng Res* **6**:1356-84.
- Elminir H K, Benda V and Tousek J (2001) Effects of solar irradiation conditions and other factors on the outdoor performance of photovoltaic modules. *J Electr Eng* **52**:125-33.
- Gupta P, Sirohi N P S and Kashyap P S (2011) Effect of nozzle pressure, air speed, leaf area density and forward speed on spray deposition in simulated crop canopy. *Ann Hortic* **4**:72-77.
- Hassan D M and Bushra E N (2010) Spray droplet number and volume distribution as affected by pressure and forward speed. *AMA* **41**: 36-42.
- Hassen S, Nasir N, Azwadi C, Jamaludin S and Sheriff M (2013) Effect of nozzle type, angle and pressure on spray volumetric distribution of broadcasting and banding application. *J Mech Eng Res* **5**:76-81.
- Jassowal N S, Singh S K, Dixit A K and Khurana R (2016) Field evaluation of a tractor operated trailed type boom sprayer. *Agric Eng Today* **40**:41-52.
- Joshua R, Vasu V and Vincent P (2010) Solar sprayer an agriculture implement. *Int J Sustain Agric* **2**:16-19.
- Kalikar V K, Prakash K V, Veerengouda M and Sushilendra (2013) Performance evaluation of bullock cart mounted engine operated sprayer. *Int J Agric Eng* **6**:101-04.
- Karale D S, Kankal U S, Khambalkar V P and Gajakos A V (2014) Performance evaluation of self- propelled boom sprayer. *Int J Agric Eng* **7**: 137-41.
- Kepner R A, Bainer R and Barger E L (1987) *Principals of Farm Machinery*. Pp 1-47. CBS Publishing Company, New Delhi.

- Kingra P K (2018) Variability analysis and empirical estimation of solar radiation at Ludhiana. *Ann Agric Res* **39**:1-7.
- Kumar M S, Balasubramanian K R and Maheswari L (2019) Effect of temperature on solar photovoltaic panel efficiency. *Int J Eng Adv Technol* **8**:2593-95.
- Li Z, Yang J, and Dezfuli P A N (2021) Study on the influence of light intensity on the performance of solar cell. *Int J Photoenergy* **2021**:1-10.
- Lu X C, Han D and Huang Z (2011) Fuel design and management for the control of advanced compression-ignition combustion modes. *Prog Energy Combust Sci* **37**:741–83.
- Majaw T, Deka R, Roy S and Goswami B (2018) Solar charge controllers using MPPT and PWM: A review. *ADBU J Electr Electron Eng* **2**:1-4.
- Mathew V J, Des S K, Das D K and Pradhan S C (1992) Development and testing of power tiller- operated boom sprayer. *AMA* **23**:25-27.
- Mishra A, Bhagat N and Singh P (2019) Development of solar operated sprayer for small scale farmers. *Int J Curr Microbiol App Sci* **8**:1-4.
- Padmanathan P K and Kathirvel K (2007) Performance evaluation of power tiller operated rear mounted boom sprayer for cotton crop. *Res J Agric and Biol Sci* **3**:224-27.
- Patil A P, Chavan S V, Patil A P and Geete M H (2014) Performance evaluation of solar operated knapsack sprayer. *Agric Eng Today* **38**:15-19.
- Poudel B, Sapkota R, Shah R B, Subedi N and Anantha Krishna G L (2017) Design and fabrication of solar powered semi automatic pesticide sprayer. *Int Res J Eng Technol* **4**:2073-77.
- Rao V V, Mathapati S and Amrapur B (2013) Multiple power supplied fertilizer sprayer. *Int J Sci Pub* **3**:1-3.
- Sharma D N and Jain M (2019) *Farm Machinery Design Principles and Problems*. Pp 209-37. Jain Brothers, New Delhi.
- Singh A K (2018) *Development and evaluation of multi-nozzle backpack type power sprayer*. M.Tech. thesis, Punjab Agricultural University, Ludhiana, Punjab, India.
- Singh J and Singh A (2013) Solar energy usefulness and its scenario : Big boon to Punjab districts. *National Conference on Electrical Systems and Energy Technologies*.
- Singh S (1996) *Studies on the spray pattern of different nozzles*. B.Tech. project report of Department of Farm Machinery Power & Engineering, Punjab Agricultural University, Ludhiana, Punjab, India.

- Singh S K, Singh S, Dixit A K and Khurana R (2010) Development and field evaluation of tractor mounted air assisted sprayer for cotton. *AMA* **41**: 49-54.
- Singh S K, Singh S, Sharda V and Singh N (2006) Performance of different nozzles for tractor mounted sprayers. *J Res Punjab Agric Univ* **43**: 44-49.
- Singh T P (2017) *Farm Machinery*. Pp 139-72. PHI Learning Private Limited, Delhi.
- Sinha J P, Singh J K, Kumar A and Agarwal K N (2018) Development of solar powered knapsack sprayer. *Indian J Agric Sci* **88**:590-95.
- Swami V, Chauhan D K, Santra P and Kothari K (2016) Design and development of solar PV based power sprayer for agricultural use. *Annals of Arid Zone* **55**:51-57.
- Swaminathan S, Mallikarjuna J M and Ramesh A (2010) An experimental study of the biogas-diesel HCCI mode of engine operation. *Energy Convers Manag* **51**:1347-53.
- Vasisht M S, Srinivasan J and Ramasesha S K (2016) Performance of solar photovoltaic installations: Effect of seasonal variations. *Solar Energy* **131**:39-46.
- Wang G, Lan Y, Yuan H, Qi H, Chen P, Ouyang F and Han Y (2019) Comparison of spray deposition, control efficacy on wheat aphids and working efficiency in the wheat field of the unmanned aerial vehicle with boom sprayer and two conventional knapsack sprayers. *Appl Sci* **9**:1-16.
- Yadav K A (2015) *Development and evaluation of bullock drawn solar powered high clearance sprayer for selected field crops*. M.Tech. thesis, University of Agricultural Sciences, Raichur, Karnataka, India.
- Yallappa D, Palled V, Veerangouda M and Sushilendra (2016) Development and evaluation of solar powered sprayer with multi-purpose applications. *IEEE Global Humanitarian Technology Conference*. Seattle, Washington, USA.
- Zhu H, Salyani M and Fox R D (2011) A portable scanning system for evaluation of spray deposit distribution. *Comput Electron Agric* **76**:38-43.
- Zilpilwar S R, Kalbande S R and Ghadge A S (2018) Development of solar cum hand operated hybrid knapsack sprayer for vegetable crops. *Int J Pure App Biosci* **6**: 748-56.

APPENDICES

APPENDIX A1

Effect of pressure on spray distribution at 45 cm height

Distance from center (cm)	Spray volume collected in channels at different pressures (ml)		
	2 kg/cm ²	3 kg/cm ²	4 kg/cm ²
30.00	0.0	0.0	1.0
27.00	1.0	1.0	1.0
24.00	1.0	2.7	2.0
21.00	1.7	3.3	3.0
18.00	2.7	6.0	3.0
15.00	4.7	13.0	13.3
12.00	8.3	15.0	17.3
9.00	18.0	26.0	28.0
6.00	24.0	27.3	30.0
3.00	23.0	24.7	26.3
0.00	23.0	26.3	30.7
3.00	26.0	29.3	35.3
6.00	16.0	18.3	23.0
9.00	10.0	11.7	20.0
12.00	3.3	6.3	13.0
15.00	2.7	4.0	10.0
18.00	2.0	3.0	5.0
21.00	1.0	2.0	2.7
24.00	0.0	2.0	1.0
27.00	0.0	1.0	1.7
30.00	0.0	0.0	1.0

APPENDIX A2

Effect of pressure on spray distribution at 50 cm height

Distance from center (cm)	Spray volume collected in channels at different pressures (ml)		
	2 kg/cm ²	3 kg/cm ²	4 kg/cm ²
30.00	0.0	1.0	1.0
27.00	1.0	1.0	1.0
24.00	1.3	2.7	2.0
21.00	2.0	5.3	2.3
18.00	3.3	8.0	5.0
15.00	8.0	17.0	15.7
12.00	11.0	17.0	20.0
9.00	19.7	26.7	30.0
6.00	21.3	25.3	30.0
3.00	21.0	24.0	30.0
0.00	23.7	25.3	33.0
3.00	22.0	25.0	36.0
6.00	14.0	16.0	16.0
9.00	9.0	11.3	19.0
12.00	4.0	7.0	10.3
15.00	2.3	4.0	5.7
18.00	1.7	1.0	5.0
21.00	1.0	3.0	2.7
24.00	1.0	1.7	1.0
27.00	0.0	1.0	1.0
30.00	0.0	0.0	1.0
33.00	0.0	0.0	1.0

APPENDIX A3

Effect of pressure on spray distribution at 55 cm height

Distance from center (cm)	Spray volume collected in channels at different pressures (ml)		
	2 kg/cm ²	3 kg/cm ²	4 kg/cm ²
36.00	0.0	0.0	1.7
33.00	0.0	1.0	1.0
30.00	1.0	2.0	2.7
27.00	1.0	4.0	2.3
24.00	1.7	4.3	3.3
21.00	2.7	12.0	7.7
18.00	4.0	12.7	11.0
15.00	8.3	16.0	18.0
12.00	9.7	14.3	19.0
9.00	16.7	23.0	27.0
6.00	21.0	24.0	28.0
3.00	19.0	20.0	24.0
0.00	18.7	21.3	30.7
3.00	21.0	24.7	29.0
6.00	16.0	16.3	19.0
9.00	12.7	13.0	15.3
12.00	5.7	6.0	10.0
15.00	3.3	3.0	5.3
18.00	2.3	2.0	4.3
21.00	1.3	1.7	3.0
24.00	1.0	1.0	1.0
27.00	1.0	1.0	2.7
30.00	0.0	0.0	1.7
33.00	0.0	0.0	1.0

APPENDIX B1

ANOVA for NMD (μm) at upper side of top canopy

Source	DF	Type III SS	Mean Square	F Value	Pr > F
Pressure	2	9225.780411	4612.890206	7.10	0.0093
Forward Speed	1	14.311250	14.311250	0.02	0.8845
Pressure*Forward Speed	2	280.249900	140.124950	0.22	0.8092
Error	12	7801.55853	650.12988		

APPENDIX B2

ANOVA for NMD (μm) at under side of top canopy

Source	DF	Type III SS	Mean Square	F Value	Pr > F
Pressure	2	7575.489644	3787.744822	17.03	0.0003
Forward Speed	1	37.267222	37.267222	0.17	0.6895
Pressure*Forward Speed	2	487.520044	243.760022	1.10	0.3655
Error	12	2669.07787	222.42316		

APPENDIX B3

ANOVA for NMD (μm) at upper side of middle canopy

Source	DF	Type III SS	Mean Square	F Value	Pr > F
Pressure	2	7596.481344	3798.240672	13.43	0.0009
Forward Speed	1	671.000556	671.000556	2.37	0.1495
Pressure*Forward Speed	2	57.458411	28.729206	0.10	0.9042
Error	12	3394.77707	282.89809		

APPENDIX B4

ANOVA for NMD (μm) at under side of middle canopy

Source	DF	Type III SS	Mean Square	F Value	Pr > F
Pressure	2	5812.747344	2906.373672	67.97	<.0001
Forward Speed	1	57.102422	57.102422	1.34	0.2703
Pressure*Forward Speed	2	213.581344	106.790672	2.50	0.1239
Error	12	513.090867	42.757572		

APPENDIX B5

ANOVA for VMD (μm) at upper side of top canopy

Source	DF	Type III SS	Mean Square	F Value	Pr > F
Pressure	2	6956.444444	3478.222222	6.43	0.0127
Forward Speed	1	0.500000	0.500000	0.00	0.9762
Pressure*Forward Speed	2	1177.333333	588.666667	1.09	0.3679
Error	12	3756.00000	313.00000		

APPENDIX B6

ANOVA for VMD (μm) at under side of top canopy

Source	DF	Type III SS	Mean Square	F Value	Pr > F
Pressure	2	12337.44444	6168.72222	19.71	0.0002
Forward Speed	1	80.22222	80.22222	0.26	0.6218
Pressure*Forward Speed	2	393.44444	196.72222	0.63	0.5501
Error	12	6492.00000	541.00000		

APPENDIX B7

ANOVA for VMD (μm) at upper side of middle canopy

Source	DF	Type III SS	Mean Square	F Value	Pr > F
Pressure	2	9489.000000	4744.500000	12.79	0.0011
Forward Speed	1	53.388889	53.388889	0.14	0.7110
Pressure*Forward Speed	2	454.111111	227.055556	0.61	0.5582
Error	12	4450.00000	370.83333		

APPENDIX B8

ANOVA for VMD (μm) at under side of middle canopy

Source	DF	Type III SS	Mean Square	F Value	Pr > F
Pressure	2	11825.77778	5912.88889	22.54	<.0001
Forward Speed	1	168.05556	168.05556	0.64	0.4390
Pressure*Forward Speed	2	353.77778	176.88889	0.67	0.5278
Error	12	3148.00000	262.33333		

APPENDIX B9

ANOVA for UC at upper side of top canopy

Source	DF	Type III SS	Mean Square	F Value	Pr > F
Pressure	2	0.66295600	0.33147800	2.41	0.1316
Forward Speed	1	0.00128356	0.00128356	0.01	0.9246
Pressure*Forward Speed	2	0.08076044	0.04038022	0.29	0.7506
Error	12	1.64865000	0.13738750		

APPENDIX B10

ANOVA for UC at under side of top canopy

Source	DF	Type III SS	Mean Square	F Value	Pr > F
Pressure	2	0.55935878	0.27967939	2.47	0.1261
Forward Speed	1	0.02094422	0.02094422	0.19	0.6746
Pressure*Forward Speed	2	0.27720411	0.13860206	1.23	0.3279
Error	12	1.35738067	0.11311506		

APPENDIX B11

ANOVA for UC at upper side of middle canopy

Source	DF	Type III SS	Mean Square	F Value	Pr > F
Pressure	2	0.14127433	0.07063717	0.85	0.4506
Forward Speed	1	0.11632272	0.11632272	1.40	0.2590
Pressure*Forward Speed	2	0.06952544	0.03476272	0.42	0.6666
Error	12	0.99420600	0.08285050		

APPENDIX B12

ANOVA for UC at under side of middle canopy

Source	DF	Type III SS	Mean Square	F Value	Pr > F
Pressure	2	0.20392844	0.10196422	2.19	0.1546
Forward Speed	1	0.00785422	0.00785422	0.17	0.6885
Pressure*Forward Speed	2	0.12804844	0.06402422	1.38	0.2900
Error	12	0.55874400	0.04656200		

APPENDIX B13

ANOVA for droplet density at upper side of top canopy

Source	DF	Type III SS	Mean Square	F Value	Pr > F
Pressure	2	7858.474444	3929.237222	38.95	<.0001
Forward Speed	1	1161.620000	1161.620000	11.52	0.0053
Pressure*Forward Speed	2	119.110000	59.555000	0.59	0.5694
Error	12	1210.52000	100.87667		

APPENDIX B14

ANOVA for droplet density at under side of top canopy

Source	DF	Type III SS	Mean Square	F Value	Pr > F
Pressure	2	761.7033333	380.8516667	40.04	<.0001
Forward Speed	1	130.6805556	130.6805556	13.74	0.0030
Pressure*Forward Speed	2	2.7477778	1.3738889	0.14	0.8670
Error	12	114.133333	9.511111		

APPENDIX B15

ANOVA for droplet density at upper side of middle canopy

Source	DF	Type III SS	Mean Square	F Value	Pr > F
Pressure	2	6133.763333	3066.881667	80.63	<.0001
Forward Speed	1	671.000556	671.000556	17.64	0.0012
Pressure*Forward Speed	2	37.221111	18.610556	0.49	0.6248
Error	12	456.460000	38.038333		

APPENDIX B16

ANOVA for droplet density at under side of middle canopy

Source	DF	Type III SS	Mean Square	F Value	Pr > F
Pressure	2	582.4677778	291.2338889	54.74	<.0001
Forward Speed	1	112.5000000	112.5000000	21.15	0.0006
Pressure*Forward Speed	2	3.8433333	1.9216667	0.36	0.7042
Error	12	63.8400000	5.3200000		

APPENDIX B17

ANOVA for area coverage (%) at upper side of top canopy

Source	DF	Type III SS	Mean Square	F Value	Pr > F
Pressure	2	62.70210000	31.35105000	5.43	0.0209
Forward Speed	1	6.30125000	6.30125000	1.09	0.3166
Pressure*Forward Speed	2	0.04990000	0.02495000	0.00	0.9957
Error	12	69.2312000	5.7692667		

APPENDIX B18

ANOVA for area coverage (%) at under side of top canopy

Source	DF	Type III SS	Mean Square	F Value	Pr > F
Pressure	2	21.63914444	10.81957222	19.32	0.0002
Forward Speed	1	1.31760556	1.31760556	2.35	0.1510
Pressure*Forward Speed	2	0.18521111	0.09260556	0.17	0.8495
Error	12	6.71966667	0.55997222		

APPENDIX B19

ANOVA for area coverage (%) at upper side of middle canopy

Source	DF	Type III SS	Mean Square	F Value	Pr > F
Pressure	2	54.23187778	27.11593889	7.12	0.0092
Forward Speed	1	9.84200556	9.84200556	2.58	0.1339
Pressure*Forward Speed	2	0.88221111	0.44110556	0.12	0.8916
Error	12	45.7118667	3.8093222		

APPENDIX B20

ANOVA for area coverage (%) at under side of middle canopy

Source	DF	Type III SS	Mean Square	F Value	Pr > F
Pressure	2	12.92410000	6.46205000	10.70	0.0021
Forward Speed	1	1.37780000	1.37780000	2.28	0.1568
Pressure*Forward Speed	2	0.18910000	0.09455000	0.16	0.8568
Error	12	7.24580000	0.60381667		

APPENDIX B21

ANOVA for ground losses

Source	DF	Type III SS	Mean Square	F Value	Pr > F
Pressure	2	0.25556400	0.12778200	9.87	0.0029
Forward speed	1	0.00405000	0.00405000	0.31	0.5863
Pressure*Forward speed	2	0.00022800	0.00011400	0.01	0.9912
Error	12	0.15542400	0.01295200		

VITA

Name of the Student : Tushar Dhar
Father's name : Parimal Kumar Dhar
Mother's name : Bina Dhar
Nationality : Indian
Date of birth : 2nd October, 1996
Permanent home address : P.O. & Vill. Khagrabari, Burirpat By Lane, Cooch Behar 736101, West Bengal

EDUCATIONAL QUALIFICATIONS

Bachelor degree : B.Tech. (Agricultural Engineering)
University : Uttar Banga Krishi Viswavidyalaya, Pundibari, Cooch Behar, West Bengal
Year of award : 2018
OCA : 8.69/10.00
Master's degree : M.Tech. (Farm Machinery and Power Engineering)
University : Punjab Agricultural University, Ludhiana
Year of award : 2021
OCA : 8.68/10.00
Title of Master's Thesis : Development and evaluation of a solar photo voltaic assisted sprayer mounted on a self propelled carrier
Awards/Fellowships/Scholarships :

- Prime Minister's Scholarship by DESW during Bachelor degree
- Gold Medalist during Bachelor degree
- National Talent Scholarship by ICAR during Master's degree